Planetary and Space Science 208 (2021) 105339

Contents lists available at ScienceDirect

Planetary and Space Science

journal homepage: www.elsevier.com/locate/pss

The Planetary Terrestrial Analogues Library (PTAL) – An exclusive lithological selection of possible martian earth analogues

Henning Dypvik [a,*], Helge Hellevang [b], Agata Krzesińska [b], Christian Sætre [c], Jean-Christophe Viennet [d], Benjamin Bultel [b], Dwijesh Ray [e], Francois Poulet [f], Damien Loizeau [f], Marco Veneranda [g], Fernando Rull [g], Agnes Cousin [h], Stephanie C. Werner [b]

[a] Department of Geosciences and Department of Technology Systems, Univ. of Oslo, P.O. Box 1047, Blindern, NO 0316, Oslo, Norway
[b] Centre for Earth Evolution and Dynamics, Department of Geosciences, Univ. of Oslo, Norway
[c] Norwegian Geotechnical Institute, Trondheim, Norway
[d] Institute de mineralogie, de physique des materiaux et comochimie, IMPMC, Sorbonne University, Paris, France
[e] Physical Research Laboratory, Ahmedabad, India
[f] Institute of Space Astrophysics, CNRS/ Paris-Sud University, France
[g] Department of Condensed Matter Physics, Crystallographie and Mineralogie, Universidad de Valladolid, Spain
[h] Institut de Recherche en Astrophysique et Planetologie, IRAP, University of Toulouse, France

ARTICLE INFO

Keywords:
Terrestrial analogues
Lithological and mineralogical background information

ABSTRACT

The Planetary Terrestrial Analogues Library (PTAL) is a dedicated lithological collection that currently consists of 102 terrestrial rock samples selected to be possible Mars analogues. The ultimate goal is improving future remote mineralogical and petrological analysis on Mars and other planetary bodies based on selected analysis such as Near- Infrared Reflectance Spectroscopy (NIR), Raman spectroscopy, Laser Induced Breakdown Spectroscopy (LIBS) and X-ray diffraction (XRD).

Most international standards applied in the remote martian mineralogical and petrological analysis have so far been based on single, pure mineral analysis, with minimal interferences from other naturally occurring minerals. Here we present detailed lithological sample evaluations based on field appearance along with optical and XRD analysis of key terrestrial rock types. The detailed mineralogical and petrological descriptions give good basis for more complete lithological understanding. In combination with NIR, LIBS and Raman analysis of the very same samples PTAL aims at improving mineralogical and petrographical information from future rovers on Mars e.g. NASA's Mars2020-Perseverance and ESA and Roscosmos's ExoMars - Rosalind Franklin.

The PTAL sample collection covers exclusively collected volcanic, magmatic and various sedimentary rocks and regoliths from well-known locations all over the world. These samples have a general composition comparable to what is currently known from Mars. The strength of this sample collection is its origin as common whole rock samples, in which minerals occur in their natural settings. It thereby allows studying possible detection interferences and a comparison of the sensitivity of the different techniques. The collection, in addition, forms the base for various alteration studies to better understand and explain alteration and weathering conditions on Mars.

The complete results and sample preparations will be available to all scientists interested.

1. Introduction

The aim of the Planetary Terrestrial Analogues Library (PTAL) project was to build and exploit the spectral library for the characterization of the mineralogical and geological evolution of terrestrial planets with emphasis on Mars. Therefore, we collected and characterized terrestrial rocks as analogues, which could support investigations of the heterogeneous, martian crust and define a wide range of its alteration products

* Corresponding author.
E-mail addresses: henning.dypvik@its.uio.no (H. Dypvik), helge.hellevang@geo.uio.no (H. Hellevang), a.m.krzesinska@geo.uio.no (A. Krzesińska), christian.setre@ngi.no (C. Sætre), jean.christophe.viennet25@gmail.com (J.-C. Viennet), benjamin.bultel@geo.uio.no (B. Bultel), dwijeshray@gmail.com (D. Ray), francois.poulet@universite-paris-saclay.fr (F. Poulet), damien.loizeau@universite-paris-saclay.fr (D. Loizeau), marco.veneranda87@gmail.com (M. Veneranda), rull@fmc.uva.es (F. Rull), agnes.cousin@irap.omp.eu (A. Cousin), stephanie.werner@geo.uio.no (S.C. Werner).

https://doi.org/10.1016/j.pss.2021.105339
Received 4 February 2021; Received in revised form 1 September 2021; Accepted 3 September 2021
Available online 11 September 2021

Fig. 1. World map with sampling sites marked by red circles. See Table 1 and www.ptal.eu.

and regoliths, thereby enhancing the evaluation of habitability potential. We mainly set out to collect natural rock samples analogous to the rocks suggested to be present at the martian landing sites with the purpose of:

1) characterizing rocks and their naturally occurring alteration products as input for the spectral library with standard commercial and dedicated spacecraft instrumentation (NIR, RAMAN, LIBS, XRD) under laboratory conditions, and where possible on in-situ field campaigns at Earth sites analogue to the diversity of the old martian unaltered and altered crust (Lantz et al., 2020; Loizeau et al., 2020; Veneranda et al., 2019a and b, 2020, 2021), and
2) performing laboratory experiments under controlled conditions and documenting rock alteration of these field-collected materials, so that the impact of varying environmental conditions (e.g., gas pressure, temperature, pH-value) can be quantified (Viennet et al., 2017; Sætre et al., 2018). After experiment completion, resulting products were characterized using standard commercial and dedicated spacecraft instrumentation (NIR, XRD, SEM-EDS). The alteration products generally consist of fine grained, clayey material and are stored with the whole rock sample collection. To insure that the geochemical reactions were at equilibrium, the altered aqueous solution were analysed regularly (~every day). The experiments were stopped and then analysed, when the chemical analysis reached a plateau (Viennet et al., 2019a and b). All details are described in separate publications and alteration stage at termination presented.

The PTAL purpose is not to provide direct analogues to the various landing sites, but to collect protoliths that are comparable of what to be found on Mars or results martian alteration. PTAL has focussed on the regions of Mawrth Vallis and Oxia Planum.

All characterized samples are documented in a publicly available online database, which will allow users to jointly interpret laboratory results and newly gathered in-situ or remote sensing data using the same or similar spacecraft instruments for various techniques (LIBS, NIR, RAMAN) on board of current and future space missions (e.g. Mars Science Laboratory, Mars2020, Tianwen, ExoMars2022). The PTAL library is organized as a modern file handling system with search and simple data manipulation tools, sorted along with the individual sample. Accessible links to the database are provided at www.ptal.eu, and the PTAL platform will be ready to be released to public from the end of the project; September 30th, 2021.

The proposed list of samples reflects the knowledge of remotely-sensed typical martian rock types, and those to be found at some of the rover landing sites. All samples are characterized based on field appearance and standard optical microscopic descriptions, along with LIBS/NIR spectroscopy and Raman analysis. X-ray diffraction (XRD) provides the crystallographic information about the chemical bonds and non-covalent interactions, whereas scanning electron microscopy (SEM) and optical microscopy provides information about the sample texture, chemical composition, as well as crystalline structure and orientation and relations of materials making up the sample. This characterisation reveals the detectability of minerals by the different methods carried on the rovers.

Although no place on Earth is truly like Mars, several sites on our planet may approximate martian conditions in some specific ways, in terms of geological processes, mineral transformation and environmental conditions. The terrestrial analogue sites may apply to either present or past conditions on Mars. The preselection of the samples to be collected was strongly driven by rock types and geological settings of Mars in general and the specific landing site candidates for the ESA's ExoMars and NASA's Mars 2020 missions, as well as the actual landing sites chosen. This current sample collection is described in more detail in the following.

In total 102 different sample types of major comparable martian lithologies were collected at 31 localities in 8 countries (Fig. 1, Table 1). The samples were analysed and the data are provided in a publicly available database. Some of selected samples are applied in alteration experiments (Viennet et al., 2017; Sætre et al., 2018; Bultel et al., 2019) following precursor work of Declercqe et al. (2009) and Hellevang et al. (2013). The database is open to additional samples with the premise of providing, besides the mineralogical and petrographical characterization, also the spectral characterization using space-dedicated

Table 1
Sample overview rock types in the PTAL collection.

Dypvik et al., Table 1, sample overview		
Sample overview; impactites, volcanics, ultramafics		
Geological setting	Lithologies	Localities
Impactites	Impact melt	Gardnos, Vredefort, Lonar
	Suevite	Chesapeake Bay
	Impact breccia	Vista Allegre, Vargeao Dome, Lonar
Volcanics	Basanite	Gran Canary, Tenerife
	Tephriphonolite	Gran Canary
	Phonolite	Tenerife
	Volcaniclastic	Gran Canary, Tenerife, John Day Valley
	Hyaloclatite	Gran Canary
	Pumice/basanite	Gran Canary
	Tholeiite –sand, lava	Leka, Reykjanes
	Basalt, alkali olivine basalt	John Day Valley, Gran Canary
	Rhyolite	John Day Valley
	Andesite	John Day Valley
	Ferripicrite	Rum, Reykjanes
Ultramafic rocks	Gabbro	Ullernaasen, Brattaasen
	Harzburgite	Leka
	Dunite	Leka
	Chromite	Leka
	Gabbro	Leka
	Serpentine cgl.	Leka
	Pyroxenite	Antarctica
Sample overview; hydrothermal and altered rock samples		
Geological setting	Lithologies	Locality
Hydrothermal rocks	Solfatara	Reykjanes
	Weathering horizons	Rio Tinto
	Weathering horizons	Jaroso Ravine
Altered volcanics	Altered phonolite	Gran Canary, Tenerife
	Altered basalt	John Day Valley
	Altered rhyolite	John Day Valley
	Altered andesite	John Day Valley
Paleosols	Oxisol, andisol, Ultisol, alfisol	John Day Valley
Altered sediments	Altered schists	Otago

instrumentation of the NIR, LIBS and Raman techniques. Currently sample types of specific mineralogy, such as sulphates, zeolites and meteorites in general are scarce in the present collection. However, we have focused on the protoliths, and dedicated alteration experiments in controlled environmental conditions to avoid biological medation or any bias of the terrestrial atmosphere composition in the alteration processes. We have addressed the mineral assemblages formed due to aqueous alteration in the experiments, which have been documented in several separate papers (Viennet et al., 2017, 2019a and b, Bultel et al., 2019, Sætre et al., 2018, Veneranda et al., 2020, 2021, and Krzesinska et al., 2021).

The composition of the martian igneous crust is likely more complex than classically assumed being dominated by sub-alkaline basalt composition (McSween et al., 2009). The record of aqueous alteration of this crust is potentially as diverse as the record of alteration on Earth. The diversity of secondary mineral associations most likely reflect the diversity of water-related processes such as: precipitation/evaporation in lakes and basins, pedogenesis, diagenesis, hydrothermal processes (linked to impact crater formation or heated aquifer), metasomatism, metamorphism and possibly deuteric alteration (Bibring et al., 2005; Gendrin et al., 2005; Poulet et al., 2005; Squyres and Knoll, 2005; Mustard et al., 2008; Murchie et al., 2009; Morris et al., 2010; Michalski and Niles, 2010; Carter et al., 2013, 2015, Meunier et al., 2012; Squyres et al., 2012; Nachon et al., 2014; Michalski et al., 2015). Each of these processes has potential to drive the alteration towards different mineral assemblages, when affecting different protolith. Considering limitations of current orbital techniques in detection of felsic minerals, it is likely that the complexity of processes operating in martian crust is broadly underestimated (Carter and Poulet, 2013). The problem is further increased by a common application of mono-mineral spectral analogue databases (or artificial mixtures of minerals) to interpret spectra remotely sensed for martian lithologies. Current spectral analogue libraries are compared to data representing whole rock composition. This may result in an underestimation of some minor minerals that cannot be observed directly. Although these problems are present at all scales of investigation, it is even more important in remote sensing analysis where the mixtures occur at a meter/kilometre scale.

The PTAL is a collection of analogue rocks. It is important to emphasize that analogy refers to best mineralogical match. This analogy does not necessarily have to imply processes of formation or origin. We know for Earth that various chemical pathways, operating at different conditions, may affect rocks throughout their evolution and still manifest in similar mineral composition of final rocks. Therefore, analogue in understanding of this collection is to designate similarity in signal (for all instruments) of the whole rock due to the mineralogical association and configuration (nature of the mixture and crystallinity of minerals). Our definition of analogue used here signify that the rock compositions investigated in PTAL are not directly linked to specific processes. Rather, the different analogues were picked to provide optimal signal interpretations while the possible formation or alteration processes can be related only to the terrestrial geological setting. Its applicability to Mars requires the investigation of the geological setting of the region in which these minerals are detected on Mars. The strength of the PTAL library is that it is being built with data derived from the instruments that will be used in the next generation rover missions on Mars (Bibring et al., 2017; Korablev et al., 2017; Rull et al., 2017; Wiens et al., 2017). The results can certainly serve as a base for exploration of other bodies in the Solar System.

1.1. The martian geology and mission targets

Mars is primarily a basaltic planet with rocks exposed on its surface, commonly being of igneous origin (e.g. McSween et al., 2009). Mineral and chemical composition of martian crust have mostly been investigated by the combination of martian meteorite analyses and remote sensing techniques from orbit and complemented with in-situ analysis by rovers. The latter provides excellent and detailed data, yet only local information, while global datasets of wider range are gathered from orbital analyses. As for now, orbital data are the most comprehensive source of accessible martian mineralogical information. These orbital investigations tend to highlight predominance of mafic minerals, such as olivine and pyroxene (discerning low and high calcium pyroxene; hereafter abbreviated LCP and HCP respectively) in the martian crust (Ody et al., 2012), suggesting generally mafic or ultramafic character of martian rocks. Additionally, olivine – the mineral proxy of ultramafic rocks – reaches locally up to 20% and even higher of the martian surface rock composition (Poulet et al., 2009; Riu et al., 2019). The martian basalts have been classified (following Irvine and Baragar, 1971) as e.g. picritic basalts and komatiites, but commonly as basalts/basaltic andesite or andesite. Riu et al. (2019) also report that minerals such as plagioclase are present on martian surface in amount equal to or even higher than pyroxenes (50-40%).

Felsic components are relatively difficult to detect with NIR techniques (Poulet and Erard, 2004), but several studies report on exposures of plagioclase-dominated, anorthosite-like material (Carter and Poulet, 2013; Wray et al., 2013). Furthermore, the existence of even more silica-enriched rocks on Mars has been confirmed by in-situ analyses, e.g. alkali basalt to trachyte and granodiorite-like materials like terrestrial tonalite–trondhjemite–granodiorite (TTG) (Sautter et al., 2015, 2016, 2016; Edwards et al., 2017).

Recent remote-sensing and in situ findings on Mars broadly agree with results gained by analysis of martian meteorites. Despite that the majority of martian meteorites, based on their chemical composition,

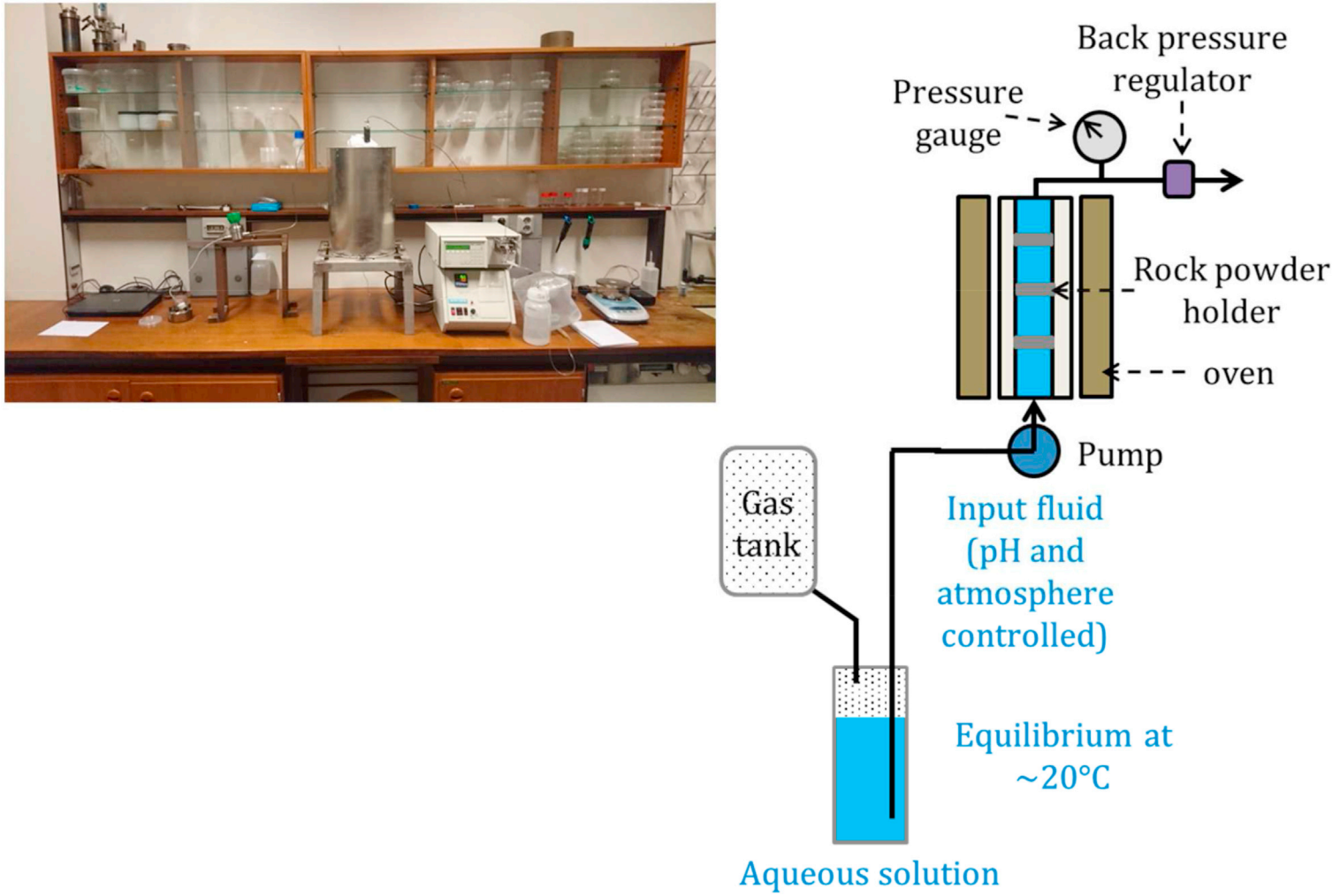

Fig. 2. Experimental set up batch/flow through ©Parr reactor, Department of geosciences, University of Oslo.

Sample: VR16-0001
Lithology: Impact melt
Weight: 130 g
Location: Leeukop Quarry, Vredefort Crater, South Africa
Degree of weathering #1

XRD analysis:
The XRD runs show large amounts of quartz, plagioclase (albite, andesine, anorthite), small amounts of orthoclase, minor amounts of illite/biotite, amphibole (?hornblende?) and dolomite.

Thin section description:
It is completely recrystallized and dominated by plagioclase but also myrmekittic intergrowth of quartz and feldspar. Small crystals of amphibole (hornblende?) and biotite (Fe-rich) are present in-between the large feldspar crystals. Small amounts of dolomite are also seen.

Fig. 3. Example of PTAL sample sheet/sheets, illustrating sample formation and basic petrographical and mineralogical descriptions, along with overview results of bulk XRD analysis. It should be noted that the sample sheet collection includes photographs and LIBS/Raman/NIR spectra. The samples are stored in the University of Oslo, while the spectra are to be found in the University of Valladolid (www.ptal.eu).

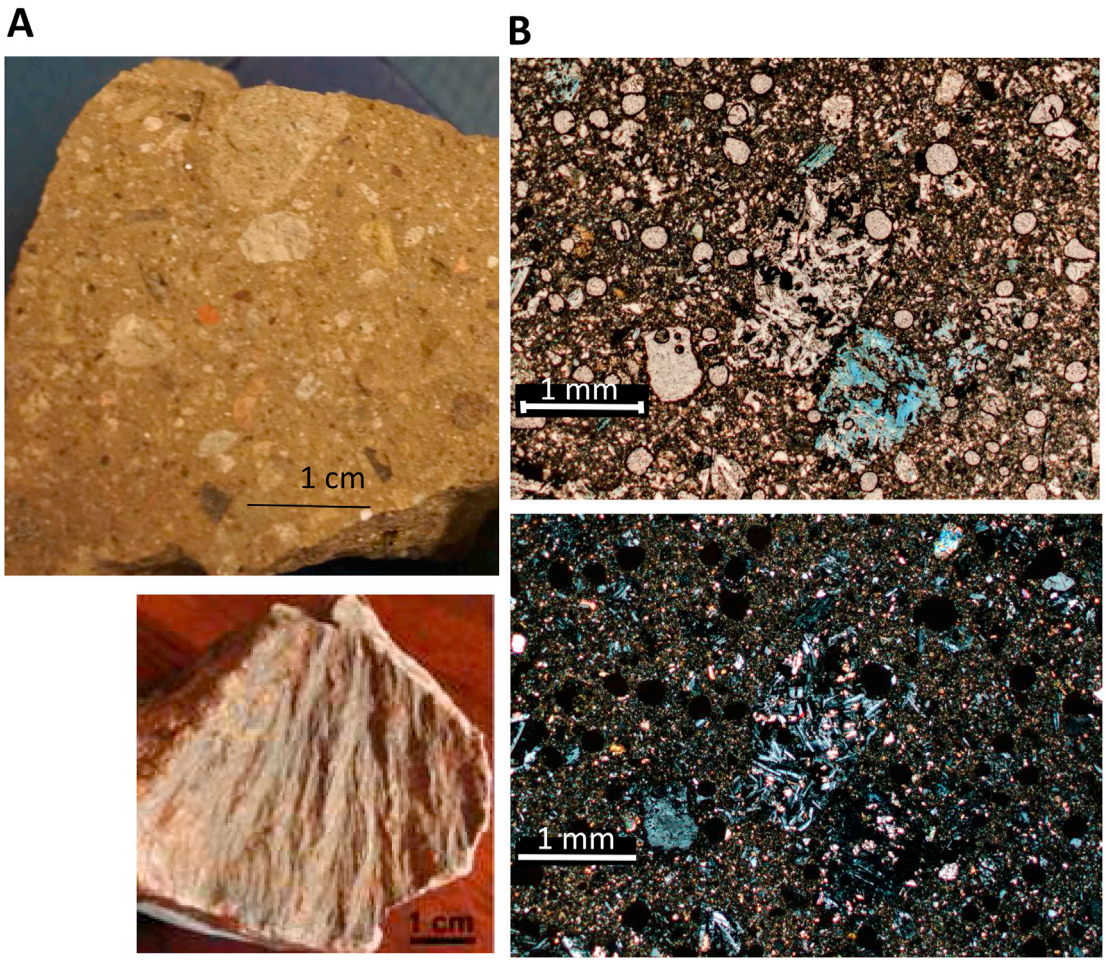

Fig. 4. A) Sample VO16-0001 from Vargeao Dome, Brazil and field photo of shatter cones from Crosta et al. (2012). B) Thin section (blue stained epoxy) photos (upper photo ordinary light, lower photo crossed polarizers) of sample VO16-0001 from Vargeao Dome, Brazil. Scale bar in photos.

indeed fall into categories of ultramafic and mafic rocks (e.g., Lodders, 1998; Papike et al., 2009), some basaltic shergottites contain late-stage mesostasis of granite-like composition (Filiberto et al., 2014; Udry et al., 2017) and nakhlite K-rich mesostasis can be connected to evolved differentiation processes (Viennet et al., 2020). This suggests that magma fractionation and formation with evolved silica-rich compositions may have occurred on Mars. Furthermore, martian basaltic breccias such as the paired specimens NWA 7034 and NWA 7533, contain a significant fraction of mm- to cm-sized igneous clasts that reveal mineral compositions characteristic of andesitic and noritic-monzonitic suites, or even trachytes (Humayun, 2013; Santos et al., 2015; McCubbin et al., 2016; Hewins et al., 2017). The origin of evolved martian lithologies is, however, still not fully understood and remains debated.

Investigations by remote sensing, in situ rover studies and analyses of meteorites indicate that the martian crust contains more Fe and Mn in bulk (and lower Mg/Si) compared to the Earth (Dreibus and Wänke, 1985; Taylor, 2013). Most importantly, based on rock compositions derived from orbital spectroscopy as well as basaltic meteorites (McSween et al., 2009), the martian surface is interpreted to be dominated by rocks of subalkaline suites. However, since the martian mantle is rich in alkalis (Dreibus and Wänke, 1985; Trønnes et al., 2019), geochemical models suggest that rocks of alkali-magma suites should be present on the surface of Mars (e.g., Carter and Poulet, 2013).

A large fraction of the martian surface is suggested to be older than 3.8 Gyrs (Noachian surface comprises roughly 60% of the surface, Tanaka et al., 2014). However, whether these ancient terrains are primary crust or younger volcanic units is also still debated. As such, composition of primary martian crust is not known and, furthermore, it is not entirely understood whether primary crust is buried beneath the volcanic terrains or is remolten. However, insight into the oldest crust composition can be obtained from analysis of impact craters. Results of such studies (Flahaut et al., 2011; Skok et al., 2012) point at the presence of LCP-rich primitive crust and younger crust being more HCP-rich. The high-calcium varieties (e.g. augite) are often associated with younger volcanic strata, while the low-calcium forms (e.g. enstatite) are more common in old highland terrains (Mustard et al., 2005). This trend is also confirmed by analysis of the global remote sensing dataset (Riu et al., 2019) and is reflected in composition of the ALH 84001 meteorite (e.g. Mittlefehldt, 1994; Papike et al., 2009 and references therein).

Mars has been a wetter planet in its earliest periods, known from geomorphological and mineralogical evidence (e.g. Howard et al., 2005; Goudge et al., 2012; Williams et al., 2013). Therefore, a part of martian surface mineralogy and composition results from water-rock interactions. A wide range of secondary minerals has formed due to interaction of the crustal rocks and water. The mineral associations include various combinations of clays that can be Al-, Al-Fe, Fe,Mg- or Mg-rich, carbonates (Ehlmann et al., 2008; Bultel et al., 2019), sulphates (Thollot et al., 2012; Flahaut et al., 2015; Weitz et al., 2011), zeolites, hydrated silica (Carter et al., 2013; Dehouck et al., 2012; Ehlmann et al., 2009), and iron oxides (Gendrin et al., 2005; Massé et al., 2008). The specific combination of mineral assemblages suggests varying water-rock interactions on Mars. Martian alteration products observed by remote-sensing methods are heterogeneous, and show the largest variety in Noachian terrains that exhibit a significant part of water-related mineralogy present on the planet (Carter, 2012). The presence of above-mentioned alteration minerals on the martian surface is confirmed by studies of meteorites, especially of nakhlites. This group of meteorites contain assemblages of Fe, Mg-clays, Fe, Mg- and Mn, Ca-carbonates, Ca-sulphates and halides (Bridges and Grady, 1999; Changela and Bridges, 2010; Lee et al., 2015). However, nakhlites are suggested to be excavated from a lava pile, and associations of alteration minerals found in nakhlites vary from sample to sample and furthermore, the distribution of elements among the various minerals is not constant (Changela and Bridges, 2010). The Noachian-aged orthopyroxenite, ALH 84001, contains carbonates that form *rosettes* with zonal Ca, Fe, Mg, Mn-composition (e.g. Borg et al., 1999; Corrigan and Harvey, 2004; Moyano-Cambero et al., 2017).

The origin of carbonates is not fully agreed upon (e.g. Valley et al., 1997; Warren, 1998; Brearley, 1998; Treiman et al., 2002; Corrigan and Harvey, 2004; Moyano-Cambero et al., 2017), and in contrast to the image perceived by remote sensing, the carbonates are not found associated with clay minerals. Most of the martian carbonates may have a hydrothermal origin (Ehlmann et al., 2008, 2009; Wray et al., 2013), weathering origin (Bultel et al., 2019; Mandon et al., 2020) or even a possible sedimentary origin (Horgan et al., 2020).

The oldest (Noachian) rocks are rich in olivine (Ody et al., 2012), but typically olivine could weather into clay minerals (e.g. Fe/Mg smectite/saponite/nontronite) in the presence of liquid water. Olivine can also appear together with Mg-carbonates, a possible product of olivine weathering involving aqueous or gaseous CO_2. Therefore, areas with large exposures of unaltered olivine-bearing rocks may indicate rather fresh erosion and that liquid water was not abundant since time of exposure.

Impact craters of all sizes are very common on the planets, so on Mars. More than 42.000 craters larger than 5 km in diameter exist on Mars (Barlow, 1988). Therefore, different varieties of impactites (e.g. impact breccias, suevites and melt rocks) should be abundant on Mars. Even if a variety of surface processes can remove the morphological expression of impacts, traces of the different impactites can still be present.

Sediments and sedimentary rocks are commonly identified on Mars, e.g. as fluvial and aeolian sequences, in the interior of several canyons, scree, avalanche, mass flow and lacustrine deposits within the many craters or other topographic depressions. Sedimentary successions probably also comprise much of the deposits in the northern lowlands, possible sites of fossil life to be detected. The main focus of the library is the collection of relevant protoliths, which can be viewed as the provenance lithologies for the different martian sedimentary phases, along with products of the alteration experiments (Viennet et al. 2017, 2019, 2019; Bultel et al., 2019; Sætre et al., 2018; Veneranda et al., 2020a, 2021; Krzesinska et al., 2021).

2. Analytical methods

The analytical aims were optimal field and sample descriptions for the library, and suitable sample sizes and quality. All locations sampled are described based on our fieldwork, published information, along with direct support and close involvement of local geologist experts. Complete sample descriptions and background information are given in www.ptal.eu.

The basic sample preparation, like cutting/sawing and crushing, was conducted at the Department of Geosciences, University of Oslo, Norway. The samples (normally between 200 and 400 g) were first split in different pieces, a large half was stored and not prepared any further, while the rest was processed into thin sections and different crushed (coarse (silt, sand and gravel) and fine (<2 μm)) phases. Part of the split was first cut and then crushed into sand-sized particles by applying a sling mill, then further crushed/micronized to a fine powder fraction of very fine silt and clay-sized particles. In the PTAL rock library, untreated and cut pieces are curated along with the different crushed samples fractions. The samples were photographed (www.ptal.eu). Besides the analytical base description of standard field notes, optical thin section studies and bulk X-ray diffraction (XRD) analysis, the samples have been analysed by NIR, Raman, and LIBS analytical methods commonly used in the different space programs, in both remote settings as well as by martian rovers. All these data are gathered in the PTAL library (www.ptal.eu).

2.1. Petrographic characterization with optical microscopy on thin sections and XRD analysis

Fresh cuts of each sample were made as 30 μm thin slides, so-called thin sections. The soft and poorly cemented sediments, altered rocks, porous and loose samples were impregnated with blue-stained epoxy

before thin sectioning. The samples were cut and double polished, before being studied and described for the library. The thin sections are uncovered and can therefore be used in e.g. future SEM and microprobe analysis. Thin section photos are included in the library collection.

The fine grained, homogenized micronized fractions were used in the bulk XRD analysis. The unoriented samples were run from 2 to 65° 2Θ on a Bruker D8 Advance diffractometer (40 kV and 40 mA) with CuKα radiation, without internal standards. In the identification, the Bruker's program *diffract.eva* was applied in combination with the Powder Diffraction Files of the International Center for Diffraction Data (ICDD) for peak comparison by applying the Rietveld method. The relative content of the volcanic glass was determined (with an accuracy of ±2%) by applying the full pattern fitting method of Chipera and Bish (2013)(Viennet et al., 2017, 2019a and b).

2.2. Raman spectroscopy

Raman spectroscopy is a non-destructive analytical technique that investigates the inelastic scattering (e.g., vibrational and rotational modes) emitted by a sample upon excitation with a monochromatic source (laser). Knowing that each molecule has a characteristic vibration pattern (fingerprint), the interpretation of Raman spectra is carried out by comparison with standard materials. As Raman spectroscopy can detect both organic and inorganic molecules, this technique is particularly suitable to investigate the mineralogical composition of analogue materials, as well to detect the presence of putative organic compounds within their inorganic matrix (e.g., biomarkers).

Raman analysis of PTAL samples was carried out by the ERICA research group, at the University of Valladolid, Spain. For this purpose, two types of instruments were used. The preliminary characterization of powdered samples was performed through the MicroRaman system. Assembled in the laboratory, the instrument is composed of the following commercial components: a Research Electro-Optics LSRP-3501 excitation laser (Helium–Neon) emitting at 633 nm, a Kaiser Optical Systems Inc. (KOSI) a HFPH Raman probe, a KOSI Holospec1.8i spectrometer and an Andor DV420A-OE-130 CCD detector. The Nikon Eclipse E600 microscope coupled to the system is equipped with interchangeable long WD objectives of 5×, 10×, 20×, 50× and 100×. Depending on the mineralogical heterogeneity of the sample under analysis, between 15 and 30 spectra were collected by focusing the excitation laser on the most interesting mineral grains. The operator manually selects the acquisition parameters (including acquisition time and number of accumulations), while spectra collection was performed through the Hologram 4.0 software.

Raman peak positions and intensity are not affected by temperature or pressure conditions. When comparing Raman analysis under martian and terrestrial conditions only minor differences have been registered.

Additional Raman analysis have been carried out by means of the so-called RLS (Raman Laser Spectrometer) ExoMars simulator, which is a laboratory spectrometer that provide spectra qualitatively comparable to those the ExoMars/RLS system will gather on Mars. The instrument is composed of a BWN-532 excitation laser (B&WTek) emitting at 532 nm, a BTC162 high resolution TE Cooled CCD Array spectrometer (B&WTek) and an optical head with a long WD objective of 50×. Through this configuration, the spectrometer resembles the range of analysis (70-4200 cm^{-1}), the working distance (≈15 mm), the laser power output (20 mW), the spectral resolution (6-10 cm^{-1}) and the spot size (≈50 μm) of the RLS instrument. The RLS ExoMars Simulator is also coupled to a vertical and horizontal positioner emulating the original Sample Preparation and Distribution System (SPDS) of the ExoMars rover. Furthermore, the instrument integrates the same algorithms developed for the RLS to operate autonomously on Mars, including autofocus and acquisition parameters optimization (Lopez-Reyes, 2017). Through this spectrometer, PTAL samples were analysed by simulating the operational constraint of the RLS. Thus, 39 spots per analogue were automatically analysed, this being the maximum number of spectra the RLS will collect from each martian sample. Data were acquired using a custom developed software based on LabVIEW 2013 (National Instruments).

Through the combined use of MicroRaman and RLS ExoMars Simulator system, over 5000 spectra were collected (Veneranda, 2019a). Raman data were visualized and treated by using the analytical tools of the IDAT/Spectpro, which is a software developed by the RLS team to receive, decode, calibrate and verify the telemetries generated by the RLS instrument on Mars (Lopez-Reyes, 2018). Spectra are interpreted by comparison with the RRUFF mineral spectra database (LaFuente, 2015) and our own RLS-ExoMars spectral database. Results of the Raman investigations are reported already by Veneranda et al. (2019a, 2019b; 2020).

The employed instrument (RLS Simulator) has been assembled to provide a similar SNR to the RLS-flight spare model (FS). Therefore, we are expecting the spectra collected in the lab to be qualitatively comparable to the one collected on Mars. A detailed comparison of the spectroscopic outcome ensured by RLS-Simulator and RLS-FS instruments is provided in a dedicated manuscript which is currently under review in the Journal of Raman spectroscopy (Lopez-Reyes et al., in review).

2.3. Laser Induced Breakdown Spectroscopy analyses

The Laser Induced Breakdown Spectroscopy (LIBS) spectral measurements have been performed at the Institute de Recherche en Astrophysique et Planetologie (IRAP) in Toulouse, France. The instrument used is the ChemCam/Mars Science Laboratory (MSL) replica (Maurice et al., 2012; Wiens et al., 2012). More details about the ChemCam replica can be found in Rapin et al. (2015). The experimental setup is made of two parts: the Mast Unit (MU), which corresponds to the telescope, laser and electronics, and the Body Unit (BU), which corresponds mainly to the spectrometers. The Mast Unit is hosted at −10 °C for better laser irradiance, whereas the Body Unit is at ambient temperature. The three spectrometers record the spectrum from the UV to the NIR domain (called UV, VIO and VNIR). Targets were placed at 1.7 m from the instrument, in a Mars chamber (where the Mars pressure and atmosphere are reproduced).

The LIBS technique is a rapid chemical analysis that uses a short laser pulse to create a micro-plasma on the sample surface. The light emitted by the plasma is collected and its spectrum recorded. The technique does not require any particular sample preparation. All the major elements can be detected (Si, Ti, Al, Fe, Mg, Ca, Na, K), as well as several minor/trace elements, such as H, Li, C, N, F, P, S, Cl, Cr, Mn, Ni, Cu, Zn, Rb, Sr, Ba, and Pb.

The powders used for the PTAL library have all a grain size that is lower than the ChemCam laser spot size (that is around 300 μm). Therefore, the signal obtained is the same, whatever the type of powder. For that reason, only the coarse-grained powders have been sampled with LIBS. Before analysis, samples have been prepared as follows: The powder samples were first heated for at least 2 h at 105 °C, in order to avoid later violent degassing when in the Mars chamber under vacuum. Thereafter they were placed in the Mars chamber for at least 2 h, at a vacuum pressure around 10^{-3} mbar. This step ensured that the samples did not degas much during the experiment, and that the H line observed cannot be related to adsorbed water. Finally, Mars atmosphere (96% CO_2, 2% N_2, 2% Ar) up to 6.5 mbar (±0.5 mbar) was injected into the chamber. Each sample was analysed at three different random spots with the ChemCam replica, for each spot usually up to 30 laser shots would be used. However, as the thickness of the powder was not sufficient in most cases (not enough material), so that already after a few shots the glass container was reached. For this reason, most of the powders have then been sampled using only 10 shots, and no change in signal registered due to grain size differences.

Data acquired are processed in the same way as the ChemCam data (Wiens et al., 2013), subtracting the dark, removing the noise, the continuum, and calibrating the spectrum in wavelength. The quantification step (Clegg et al., 2017) is not available with this setup (only for specific

studies, developing their own quantification), and will be reported later. At ChemCam (Curiosity), the SNR was better on Mars than in the lab, but generally SNR may be different between Mars and the lab, simply because conditions are not the same (e.g. temperature of spectrometers or different optical paths).

2.4. Near-infrared reflectance spectrometry

In the region of solar reflected light (0.3–4 μm), several minerals show diagnostic absorption bands due to vibrational overtones, electronic transitions, charge transfer, and conduction processes (Clark et al., 1990). The near-infrared reflectance spectrometry (NIR) has proven to be one of the best ways to characterize any sample in a quick and non-destructive way. This technique has been successfully applied in space exploration to remotely study planetary objects. When coupled to imaging capabilities, it provides unique clues for the history of the parent body in a geological context, in spite the difficulties of e.g. quartz and feldspar identification (Carter and Poulet, 2013).

The NIR characterization of PTAL samples therefore fits well into the context of future space exploration of Mars. The NIR registration for PTAL library consists of two steps: 1) to acquire NIR spectra with a laboratory PerkinElmer point spectrometer of all homogeneous crushed samples and 2) to characterize with the NIR hyperspectral imaging microscope MicrOmega/ExoMars2022 flight spare model all bulk samples that are heterogeneous in texture. These two NIR instruments do not aim to look at the same kind of samples. The point spectrometer Perkin is appropriate to analyse powders in which all minerals are mixed; it thus emphasizes the averaged composition of the samples over a one mm-sized spot. MicrOmega is dedicated to observing heterogeneous rocks where inclusions can be detected at the pixel size (20 μm) of the detector (Bibring et al., 2017). The spatial information provided by MicrOmega is less suitable for the crushed samples (powders) because the grain size is generally smaller than the pixel size. Consequently, we did not plan to measure systematically the powdered samples with MicrOmega, but rather cuts of the samples based on their mineralogy to show some MicrOmega observations of powder samples and to confirm that the crushing process homogenizes the composition (Loizeau et al., 2020). Specifically, the reflectance spectroscopy using the commercial setup (PerkinElmer Spectrum 100 N Fourier Transform spectrometer) was performed under ambient temperature and pressure conditions. The selected spectral resolution was 4 cm^{-1} over the range 0.8–4.2 μm, and the collecting spot size about 1 mm. The measurements protocol and the detailed analyses of the PTAL samples are specified in Lantz et al. (2020).

MicrOmega is a generic space instrument built at Institut d'Astrophysique Spatiale (IAS), Paris-Saclay University, France. This instrument was selected to characterize PTAL bulk samples at the microscopic scale in the NIR range. The main advantage of MicrOmega relative to the Perkin spectrometer consists in its capability to perform spectral imaging of samples at the spatial resolution of 20 μm, which is extremely useful for inhomogeneous bulk samples. A specific MicrOmega workbench has been developed for characterizing the numerous PTAL samples in an automatic way (Loizeau et al., 2020). The campaign of observations was held from April to June 2019 and detailed analyses are presented in Loizeau et al. (submitted).

MicrOmega operations within a chamber with dry atmosphere (N_2) and a cold instrument and cold sample, were mainly decided to create an environment more favorable to long operations with the instrument at high signal/noise ratio, as will be mostly the case on Mars. The instrument can operate outside of this chamber but the main difference is a lower signal/noise ratio. Due to the similar conditions between the laboratory chamber and the martian surface (similar instrument model, equivalent temperature of the instrument and samples), the signal/noise ratio is expected to be very comparable between PTAL data and data from the Rosalind Franklin rover.

2.5. Experimental work on mineral alteration in martian conditions

The experimental laboratory consists of four 600 mL Parr© reactors, two made in Hastelloy® steel and two in titanium, both resistant to corrosive fluids and gases. The upper temperature and pressure limits for these reactors are 250 (titanium) and 350 °C (steel), and 350 bar. These reactors can operate as stirred batch reactors or when equipped with a liquid pump and back-pressure regulator as flow-through reactors. Liquid and vapour phase sampling can be done during operation (Fig. 2). In addition to the Parr© reactors, one tubular titanium reactor was designed specifically to create chemical gradients along a flow path, and to better understand how weathering products depends on the chemical variables (e.g., pH).

The aims of the first batch of experiments were to assess to what extent water saturation affects chemical weathering of basalt, and how CO_2 in vapour and temperature may affect unsaturated chemical weathering (Sætre et al., 2018). The other study focussed on the competition between dioctahedral/trioctahedral phyllosilicate/carbonate/zeolite formation as a function of various CO_2 partial pressures in the atmosphere and water (Viennet et al., 2017). Both works furthermore explored the relative detectability of NIR compared to in-house laboratory methods such as XRD and SEM. In the experiments, a basaltic glass of tholeiitic composition (Stapafell, Iceland) served as martian analogue material.

The aim of the second batch experiments was to reproduce mineralogical analogue to Oxia Planum, ExoMars 2022 landing site. The closed-system equipment was used for this and the samples are characterized by the same methods as both, the collected natural analogues and other experimental products. The influence of water-rock composition, pH, salinity and CO_2 pressure was tested (Krzesińska et al., 2019, 2021).

The third set of experiments simulated an open system. Flow through experiments were performed, with equipment suitable to create chemical gradients along a flow path, in order to understand how weathering products in martian surface conditions depend on the solubility of material in various environmental conditions. Composition of the solution of alteration reflecting different possible density and composition of atmosphere, pH, and salinity. In the experiment, fluid was percolated through tholeiitic basalt samples distributed with a specific stratification. Alteration products were characterised in the PTAL framework separately for each stratum to understand how fluid composition is affected by dissolution and how the changed fluid influences alteration of following strata (Viennet et al., 2019a).

2.6. Sample characterisation and the level of alteration

The sample description gives a general geological overview of sample appearance, with additional emphasis on the degree of weathering and alteration. The samples have therefore visually been classified into degrees of weathering and alteration; five different classes, 1 to 5.

Class 1 is a fresh, unaltered rock, while class 5 represents an almost completely weathered/altered rock, a so-called saprolite in the case of soil weathering. In class 1 there are no visible signs of material alteration, while class 2 represents a slightly altered, fairly coherent rock, with possible discoloration on and along discontinuity surfaces. Class 3 is a moderately altered rock, and less than half of the rock material is decomposed. It is classified as a saprock in weathering sections. In class 4, more than half of the rock material is decomposed and the rock can be classified as a poorly to moderately developed saprolite in the case of weathering sections. Class 5 is completely altered, but the original rock structure is partly intact; a saprolite in weathering sections.

3. Sampling sites and locations

Based on the general geological knowledge of Mars composition and landing sites, the different analogue sites were selected for the PTAL library, not to provide analogues for the landing sites, but protoliths

similar to e.g. Mawrth Vallis and Oxia Planum (Fig. 1 and Table 1). In combination with accessibility, published information and local geo-expert's recommendations, the very best analogue sites were chosen. The sample collection display broad compositional variations and could be of interest for representing several different comparable martian lithologies (Fig. 3). The library will be updated with new samples as research progresses, and more martian and experimental/analytical knowledge is gained.

The selected analogue locations include volcanic sites, weathered volcanic and sedimentary lithologies, gabbroic sites, hydrothermal deposits, impact craters, various sands, fine-grained sediments and clay rich formations. Table 1 gives an overview of main locations and lithologies. It should be noted, that these samples are the starting point for experimental/alteration studies, in trying to approach and better understand the composition of weathered or otherwise chemically altered Mars. In the following, we present the samples and sampling sites according to rock types.

3.1. Impact crater sites

Impact craters are abundant on the surface of Mars, and as expected, plenty in old Noachian terrains. Accordingly, impact related alteration of rocks and minerals plays a role on Mars (Newsom, 1980; Allen et al., 1982; Hellevang et al., 2013). A few recent studies focus on the influence of impact processes and shock metamorphism in relation to the post-impact formation of hydrated materials (Tornabene et al., 2013; Cannon and Mustard, 2015; Michalski et al., 2017). The relationship may be two-fold, water-bearing minerals are most susceptible for damage as result of shock metamorphism (e.g. Ivanov and Deutsch, 2002). Therefore, they may be removed or significantly reprocessed in the proximity of impact structures. Simultaneously, impact is capable of releasing heat that may be enough to melt buried, subsurface ice and forming hydrothermal cells leading to precipitation of aqueous minerals locally in parts of impact structures (e.g. Osinski et al., 2013). Moreover, it is likely that the martian landing sites contain impact related material (Pan et al., 2019), even if an impact origin cannot be recognized due to post-impact

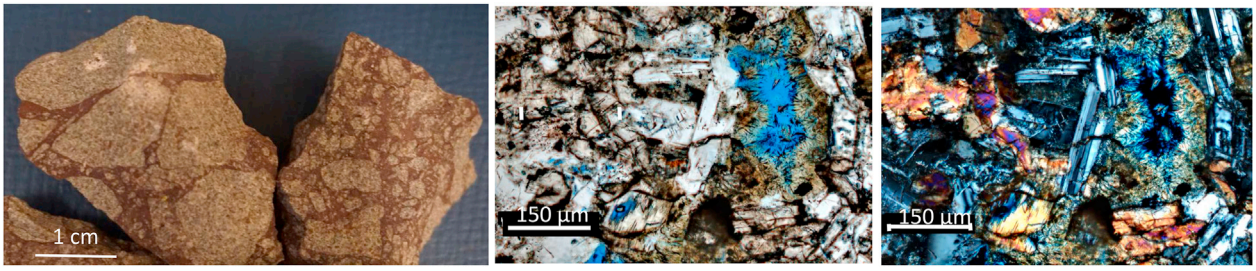

Fig. 5. Rock sample (left photo) and thin section (blue stained epoxy)(middle photo, ordinary light) of Vista Allegre sample VA 16-0001. Right photo ordinary light with crossed polarizers. Scale bar in photos.

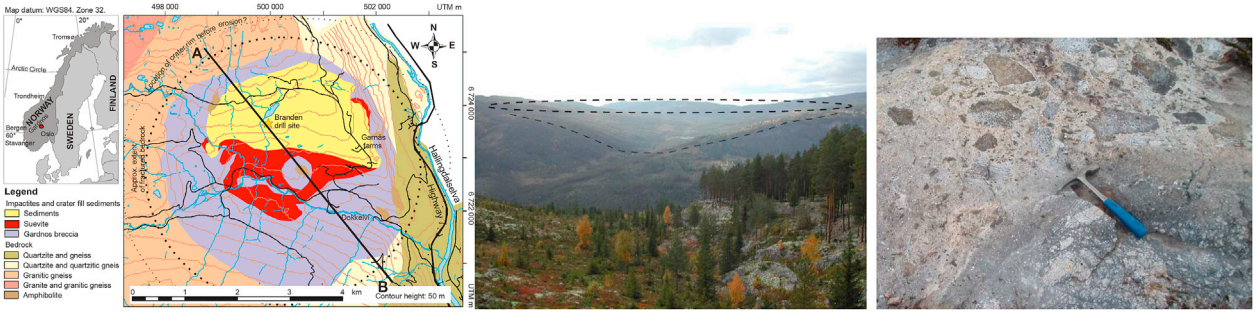

Fig. 6. Geological map of the Gardnos crater (Kalleson, 2009) and field photo with view from East towards West of the Gardnos crater (middle photo). The far right photo show outcrop of the boundary between suevite (upper left) and impact breccia (Gardnos Breccia)(lower right).

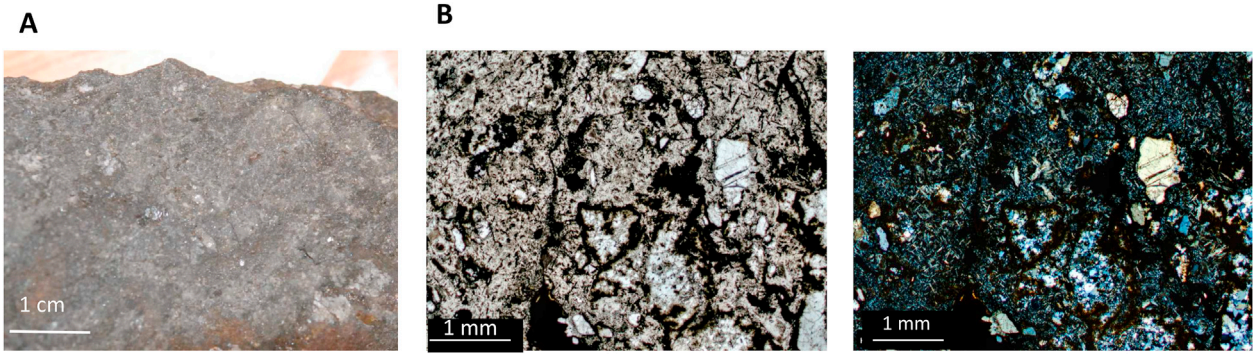

Fig. 7. A) Impact melt rock sample (GN 16-0001) of Gardnos and to the right (B) thin section photos (blue stained epoxy) of the same (middle photo ordinary light, right photo crossed polarizers). Scale bar in photos.

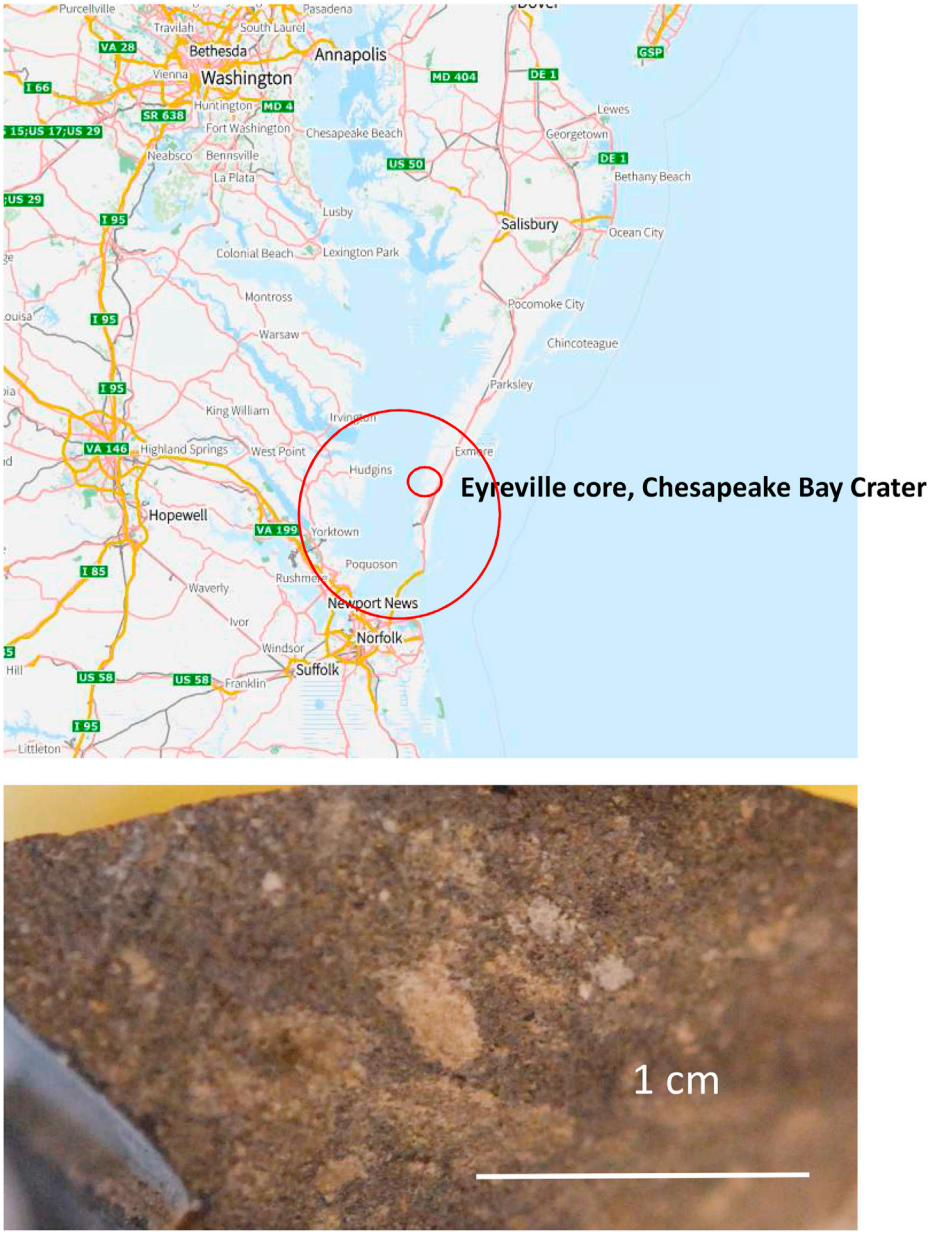

Fig. 8. Chesapeake Bay Crater map. The 85 km in diameter crater marked with a large red ring, Eyreville Core from small red ring area. The lower photo shows core sample of suevite (WH16-0014) from the Eyreville Core.

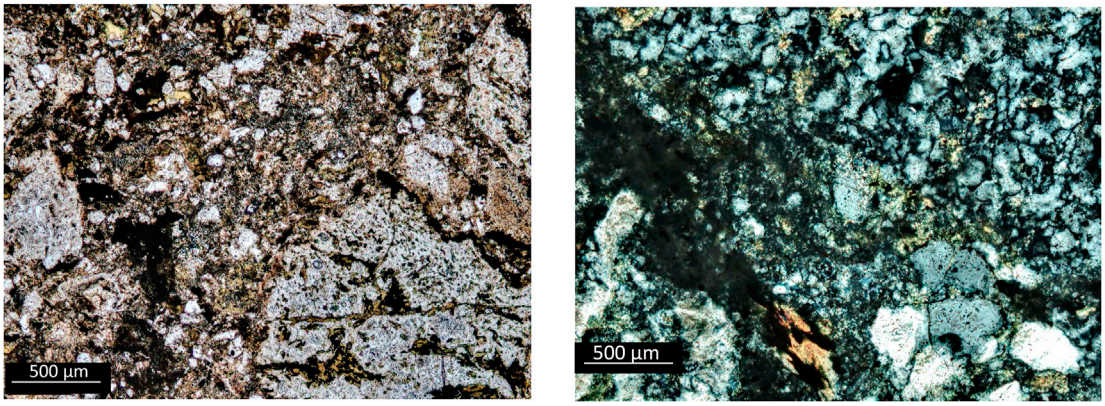

Fig. 9. Thin section (blue stained epoxy) photos of Chesapeake Bay sample WH16-0014. The thin section contains shocked quartz, not to be seen here. Left photo ordinary light, right photo crossed polarizers. Scale bar in photos.

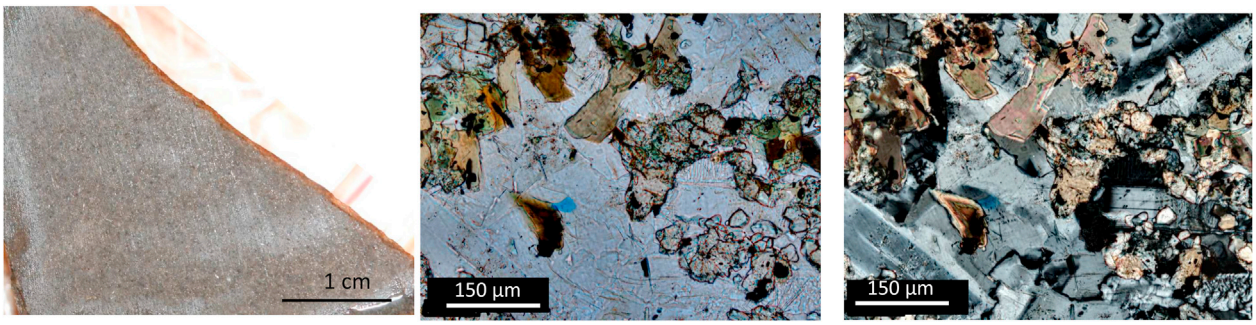

Fig. 10. Rock sample VR 16-0001 from Vredefort Crater, melt rock (to the left). Thin section (blue stained epoxy) photos to the right; middle photo ordinary light, far right photo crossed polarizers. Scale bar in photos.

geological modifications of the site. Both landing sites are densely impacted and the giant Isidis impact crater (about 1500 km in diameter) near Mars 2020 landing site also definitely show its presence e.g. with fracture systems and megabreccias (Mustard et al., 2008). Therefore, impact and shock related materials were considered for building a library that will be used in Mars studies.

Impact cratering results in obvious crater structures along with impact breccias, suevites and melt rocks, so-called impactites (French, 1998), and have been recognized in all analogue impact sites selected. The following relevant impactite samples have been included in the PTAL library (Fig. 1): impact melt (Gardnos, Norway, Vredefort, South Africa), suevite (Chesapeake Bay, USA), and impact breccias (Vista Allegre and Vargeao Dome, Brazil, Lonar, India). The latter two craters formed in basaltic terrain, which is rare on Earth, but common on Mars. The other felsic target areas (Gardnos, Vredefort, Chesapeake Bay) may possibly be more appropriate analogues for the younger martian terrains, which could include more evolved igneous rocks.

The Vargeao Dome structure is a complex impact crater (12,4 km in diameter). Its impact origin was demonstrated by Crosta et al. (2012) based on shocked quartz and shatter cones from the site (Figs. 1 and 4). The impact occurred during the Lower Cretaceous (123 ± 1.4 Ma ago) into a more than 100 m thick succession of similar aged lavas and sandstones (Serra Geral Formation) of the Parana Basin, southern Brazil. It is one of the few terrestrial craters in basaltic target rocks. The library samples from this site are different impact breccias and un-brecciated basalt.

100 km southeast to the Vargeao Dome, is the location of the Vista Alegre impact crater (Crosta et al., 2010). The diameter is a 9.5 km and 115 Ma of age. The crater samples are represented by a poorly sorted, polymict, matrix supported breccia rich in volcanic clasts from 20 μm to more than 0,5 cm in size. Plagioclase (anorthite, albite), with minor amounts of quartz, potash feldspar dominate, but dispersed minor grains of augite, diopside, saponite, stellerite (zeolite) are found along with traces of calcite and dolomite (Fig. 5).

The Lonar crater (Buldhana district, Maharashtra, India) is a simple crater, with a present day diameter of 1.9 km and depth of 150 m (Senthil Kumar et al., 2014). It was formed in the basaltic target of the Deccan large igneous province (LIP). The target rock represent tholeiite basalts crystallized at 65 Ma. The age of crater itself is not certain, but within the range of 52 and 570 ka (Sengupta et al., 1997; Jourdan et al., 2011). The impact event caused significant brecciation of the basement and formation of impact glasses that were incorporated into ejecta as spherules and impact bombs. The three samples included into PTAL collection represent target basalt, shock fractured basaltic fragment and impact melt from proximal ejecta, outside the crater rim.

The Gardnos impact structure in southern Norway (Figs. 6 and 7) is a 5 km in diameter, complex crater that has been dated to 546 Ma (French et al., 1997; Kalleson, 2009; Kalleson et al., 2009, 2010). A 250 m large impactor hit the granitic gneisses and quartzites of the Precambrian basement and created a wide selection of impactites, in the PTAL library represented by the impact melt. Goderis et al. (2009) geochemically characterized the impactor as an IA or IIIC non-magmatic iron meteorite. The Gardnos impact melt (Fig. 7) is rich in chlorite, illite, amphibole and feldspars (e.g. orthoclase, anorthite). The mineral grains are floating in a fine-grained recrystallized matrix. The grains are generally poorly sorted and spanning grain sizes from 0,5 cm down to just a few μm.

The Chesapeake Bay impact crater is a late Eocene (35.4 Ma), 85 km in diameter impact structure, which has been sampled by numerous drill cores and studied in great detail (e.g. Poag et al., 2004; Belkin and Horton, 2009; Gohn et al., 2009; Dypvik et al., 2018) (Figs. 8 and 9). The crater fill succession of the Chesapeake Bay Crater consists of large thicknesses of various mass flow deposits covering crushed basement and partly melted rocks, so-called suevites (Dypvik et al., 2018) (Fig. 8). The core samples included in the PTAL collection show fairly well preserved suevites, consisting of melt material, illite/smectite clay minerals, quartz and some minor cristoballite, along with small amounts of anorthite, sanidine and orthoclase (Fig. 9).

The more than 300 km across Vredefort Crater formed about 2000 million years ago and is the largest verified impact crater on the Earth (Gibson and Reimold, 2008). In the PTAL collection a surface sample of impact melt from the Leeukop Quarry has been included (Fig. 10). It consists of quartz, albite, anorthite, small amounts of orthoclase, illite, biotite and dolomite. In the thin section it is seen to be completely recrystallized after impact and dominated by plagioclase and myrmekitic intergrowth of quartz and feldspar. Small crystals of amphibole (hornblende) and biotite (Fe-rich) are also present in-between the large feldspar crystals.

3.2. *Volcanic igneous rocks*

A wide range of igneous rocks has been included in the library collection, e.g. tholeiitic basalts and phonolites, picrites, andesites, and basanites. Several fairly fresh volcanic formations were sampled at: Tenerife and Gran Canaria (Spain), Iceland, John Day Valley (Oregon, US), Dry Valleys (Antarctica) and Rum (Scotland) (Fig. 1 and Table 1). At Leka (Norway), altered/weathered Palaeozoic tholeiitic pillow lavas were sampled along with a broad collection of ultramafic lithologies. It is difficult to state the present degree of weathering and alteration of the basalts, but a rough evaluation can be presented based on analysing the olivine in place and the amounts of smectite present. The ultramafic samples of PTAL on the other hand vary from completely serpentinised close to unaltered. The degree and mechanisms of alteration vary and will not be reported here in detail, but has been included in the sample sheets as simple range 1–5 i.e. from unaltered (1) to highly altered (5) (see paragraph 2.6, Fig. 3).

The Holocene volcanic samples from Iceland (Fig. 1 and 11) represent the active Mid Atlantic Ridge and were sampled at localities near the cities Keflavik and Reykjavik (Einarsson, 2005; Sigmarsson and Steinthorsson, 2007). Despite being sampled in a presently active quarry, the sample interior show evidence confined of vegetation. The Icelandic

Fig. 11. Iceland location map with sampling sites on the Reykjanes peninsula.

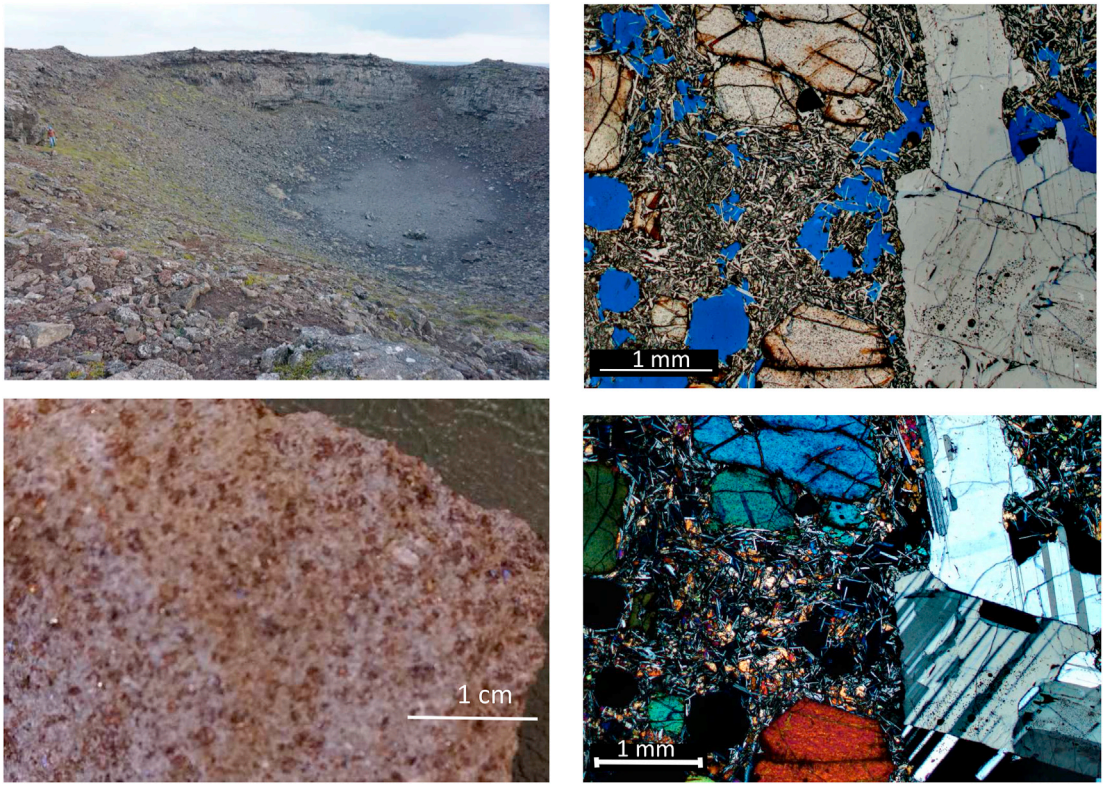

Fig. 12. The Haleyabunga crater and rock sample IS16-0001, ferropicrites (photos to the left). Thin section with blue stained epoxy to the right; upper right photo ordinary light, lower right photo crossed polarizers. Scale bar in photos.

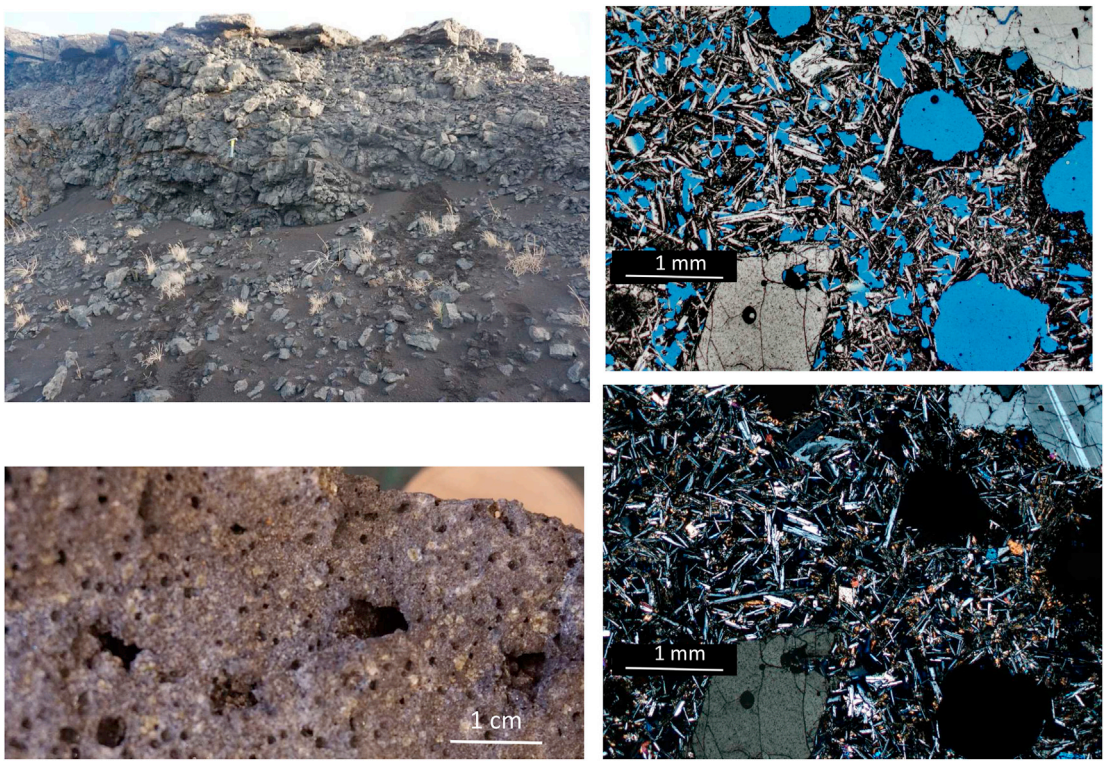

Fig. 13. Tholeiites at Stapafell, sample IS16-0008 (photos to the left). Hammer for scale in field photo, sample picked near hammer. Thin section (blue stained epoxy) (photos to the right); upper photo ordinary light, lower photo crossed polarizers. Scale bar in thin section photos.

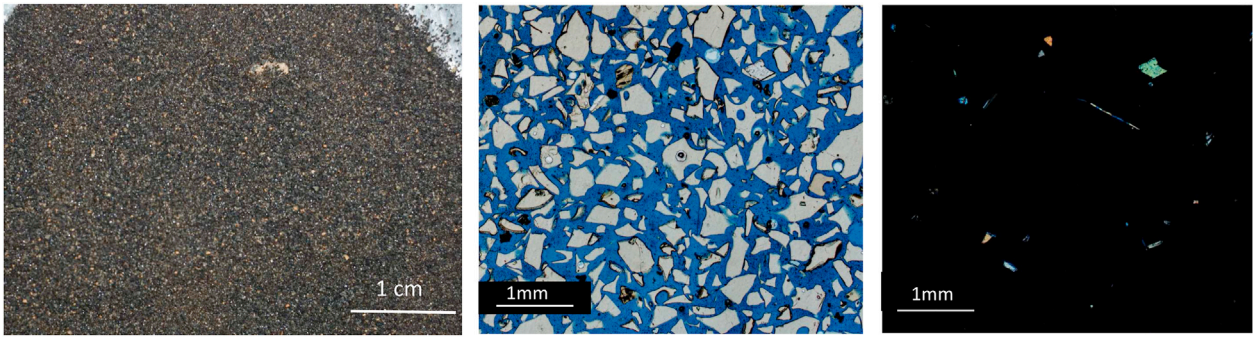

Fig. 14. Tholeiitic glass shard sand from Stapafell, sample IS16-0006, left photo. Thin section photos to the right (blue stained epoxy); middle photo ordinary light, far right photo crossed polarizers. Scale bar in photos.

samples cover ferropicrites, tholeiitic pillow lavas, tholeiitic sands in addition to the hydrothermal deposits of Seltun (Einarsson, 2005). The ferropicrites (Fig. 12) are represented by samples of generally modest degree of alteration; rich in large plagioclase, olivine and pyroxene (diopside, augite) crystals in a generally fine-grained feldspar-rich matrix. The large feldspar crystals in some cases display alteration rims. The olivine may be fragmented and somewhat altered, with hematite rims, but the secondary alteration phase has not been 100% identified. Possible garnets, but also grains of ilmenite and hematite are in addition present. Dispersed secondary pyrite and ankerite are present in voids. Some few reddish phases are seen associated with biogenic alteration with concentric Fe-oxide (silica rich) filling voids along with pore-filling zeolites (Fig. 12).

Tholeiitic pillow lavas have been sampled at Stapafell (Figs. 11 and 13). The lithology is very porous with feldspar and olivine needles. The rocks show little alteration. The main minerals are forsterite, labradorite, augite and diopside, with minor amounts of carbonates (Fig. 13).

Volcanoclastic sandstones of tholeiitic sands are common and dominated by amorphous material but grains of forsterite, quartz and feldspar (microcline, albite) are also present, along with traces of recent algae or fungi. Major alteration of glass fragments or shards are evident, some with clay coatings of smectite. Most shards are between 50 and 900 μm in size, fresh looking, angular in shape and carry vesicles (Fig. 14).

Ferropicrites and tholeiitic pillow lavas were also collected from the Eastern Layered Series, Island of Rum, NW Scotland (Fig. 15) and Dry Valleys in Antarctica (Fig. 16). The Dry Valleys sample is rich in enstatite, augite, plagioclase, and talc are found in voids (Jerram et al., 2010). The sample from Rum is a fresh surface-sample of ferropicrite with some minor alteration phases along fractures (Armstrong et al., 1978; Emelus et al., 1996). It is rich in olivine, plagioclase and carry some magnetite as well. In addition anorthite, labradorite, chlorite and possible kaolinite and smectite have been found. The clay phases are possible products of alteration (Fig. 15).

In the John Day Valley (Oregon, USA) the well-studied Columbia

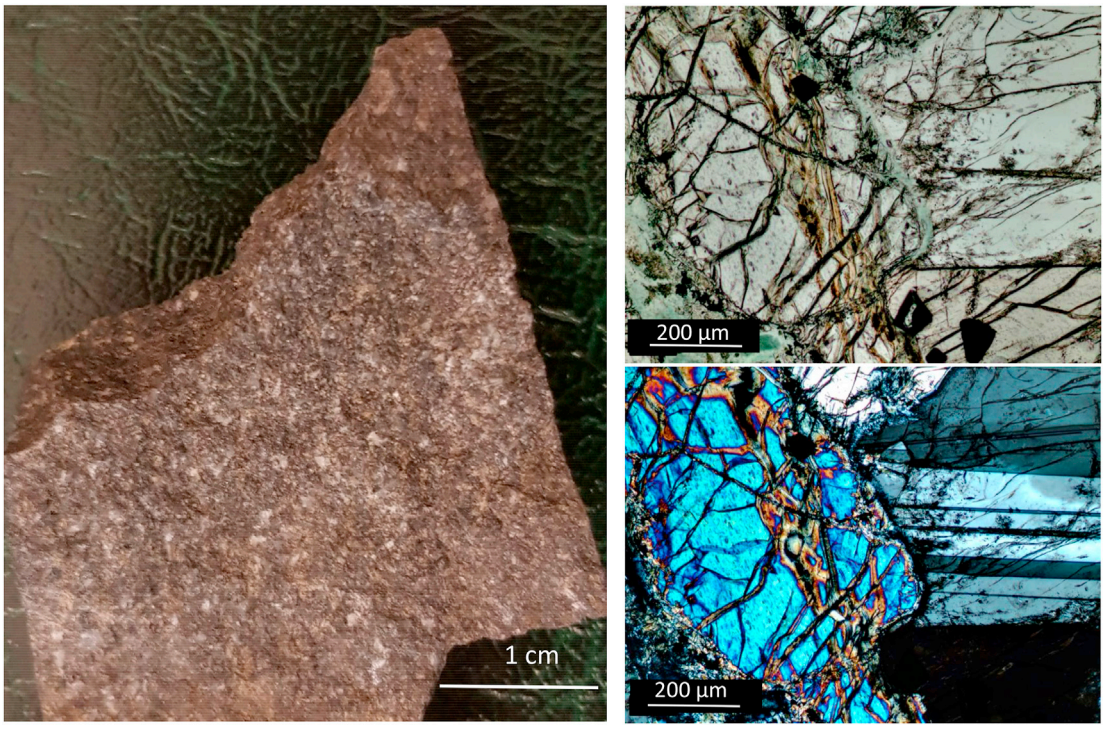

Fig. 15. Ferropicrite (RU16-0001), from Rum, Scotland (left photo). Thin sections (blue stained epoxy) to the right; upper photo ordinary light, lower photo crossed polarizers. Scale bar in photos.

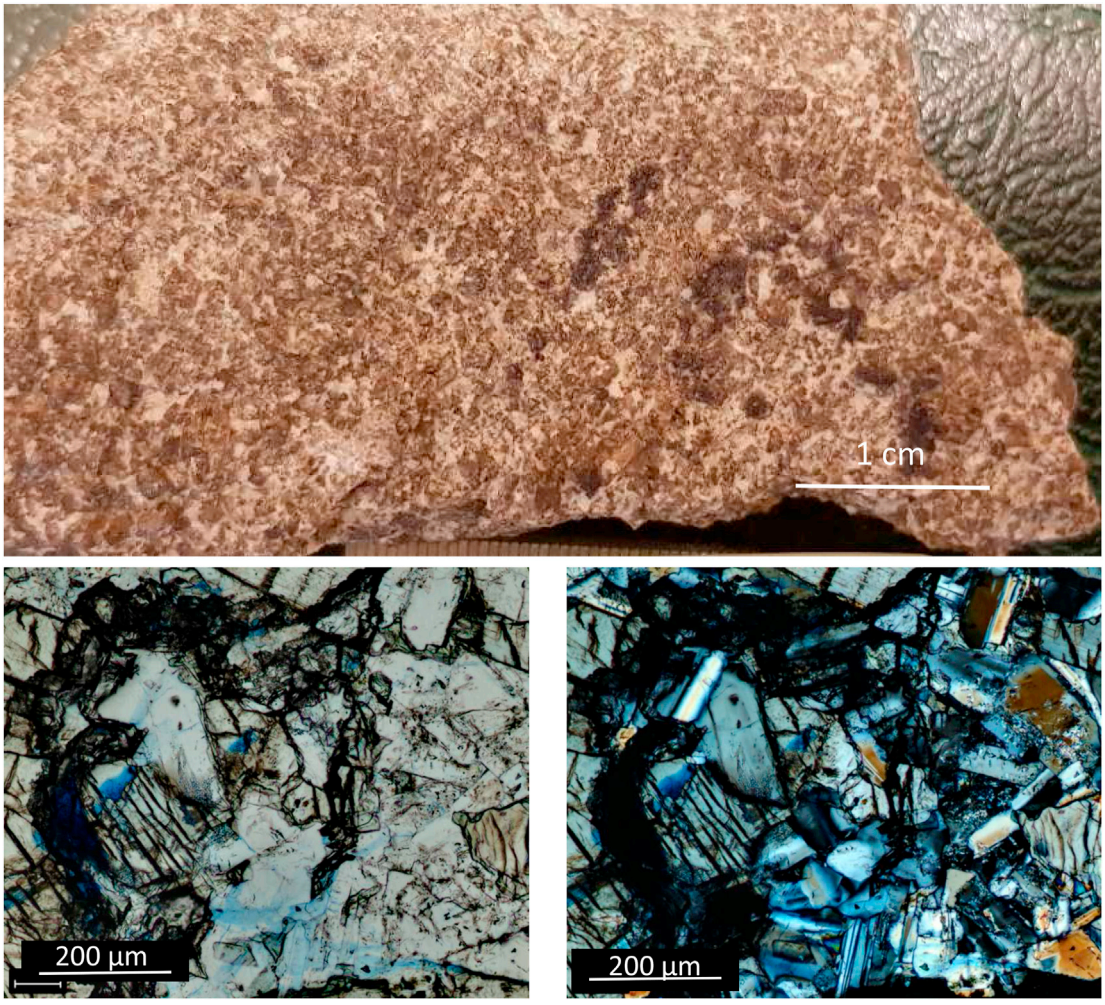

Fig. 16. Basalt from Dry Valleys, Antarctica, sample DV16-0001 (upper photo). Thin section with blue stained epoxy in lower two photos; left photo ordinary light, right photo crossed polarizers. Scale bar in photos.

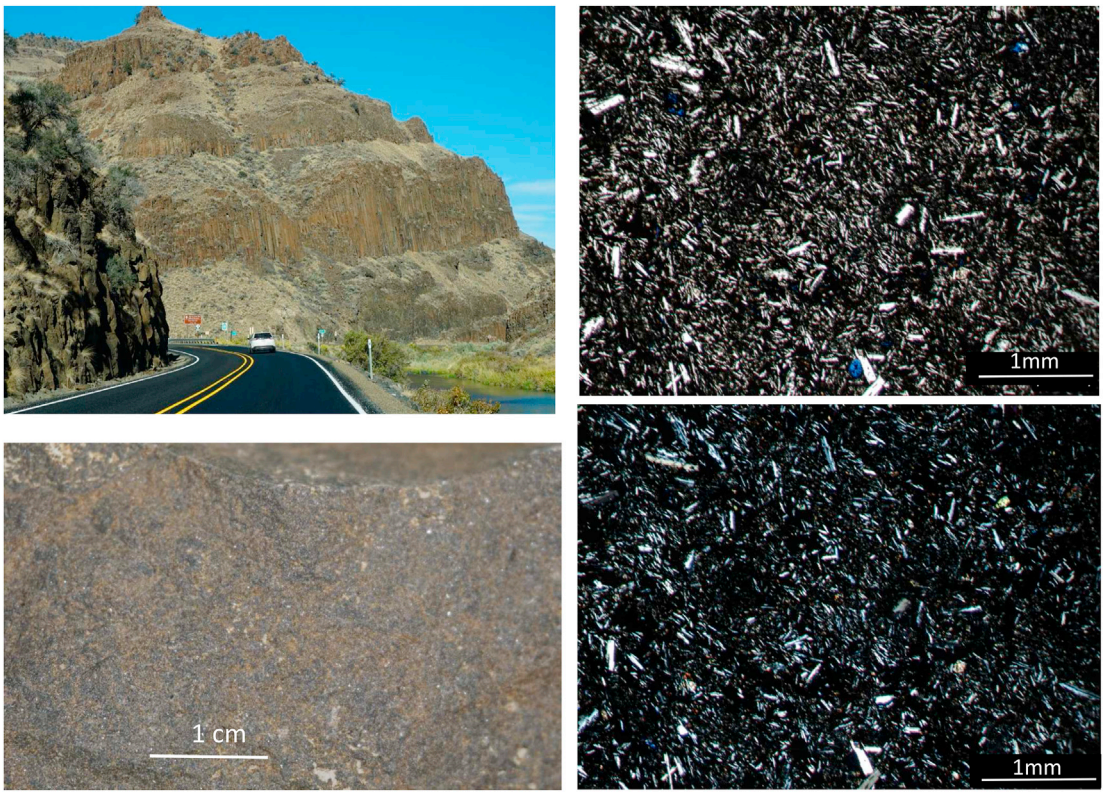

Fig. 17. In the left photos Columbia River basalt (lower left) in Picture Gorge (upper left), John Day Valley. To the right Sample JD16-0005, thin section photos, blue stained epoxy; upper photo ordinary light, lower photo crossed polarizers. Scale bar in photos.

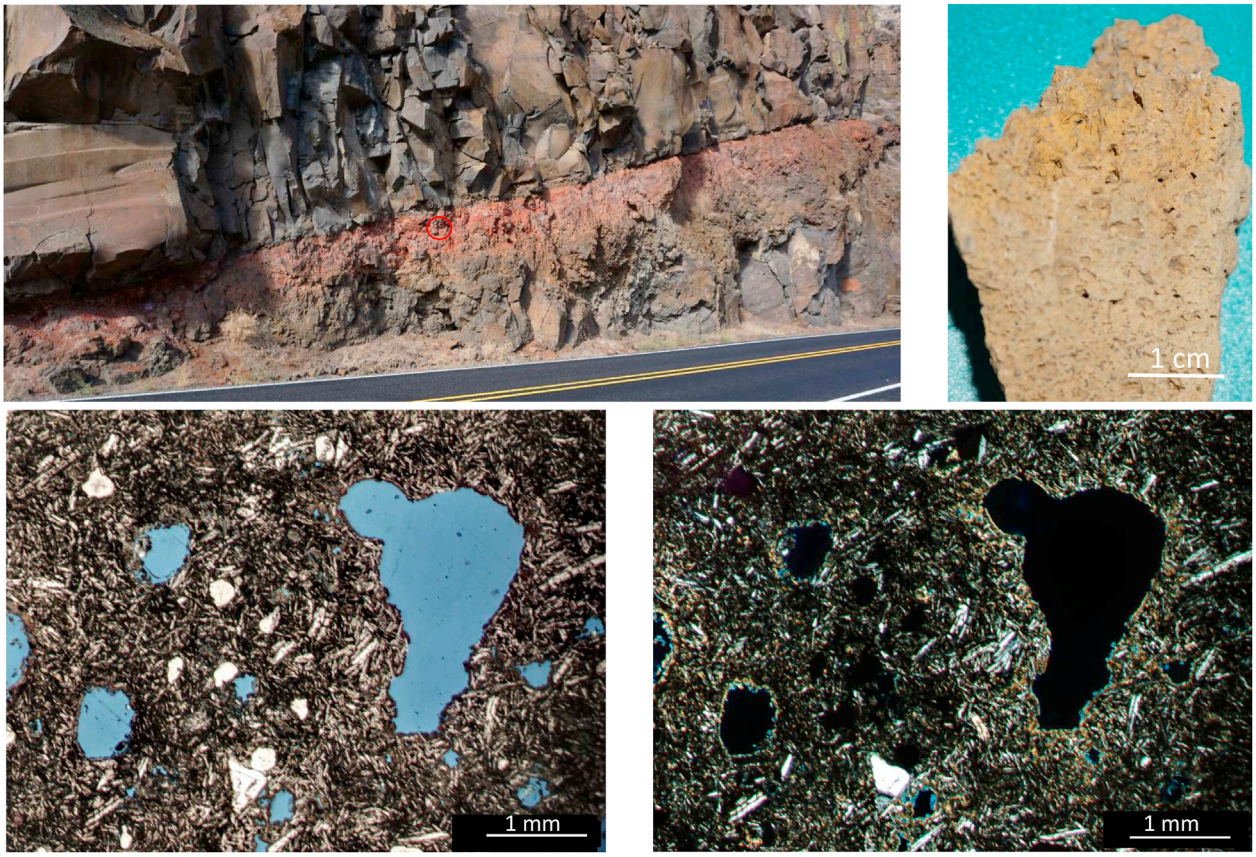

Fig. 18. Altered basalt- and unaltered Picture Gorge Basalt from John Day Valley (upper left photo). The highly altered basalt sample are shown in the top right photo (JD16-0004). Thin sections, blue stained epoxy in lower two photos; left photo ordinary light, right photo crossed polarizers. Sample at red circle. Scale bar in photos.

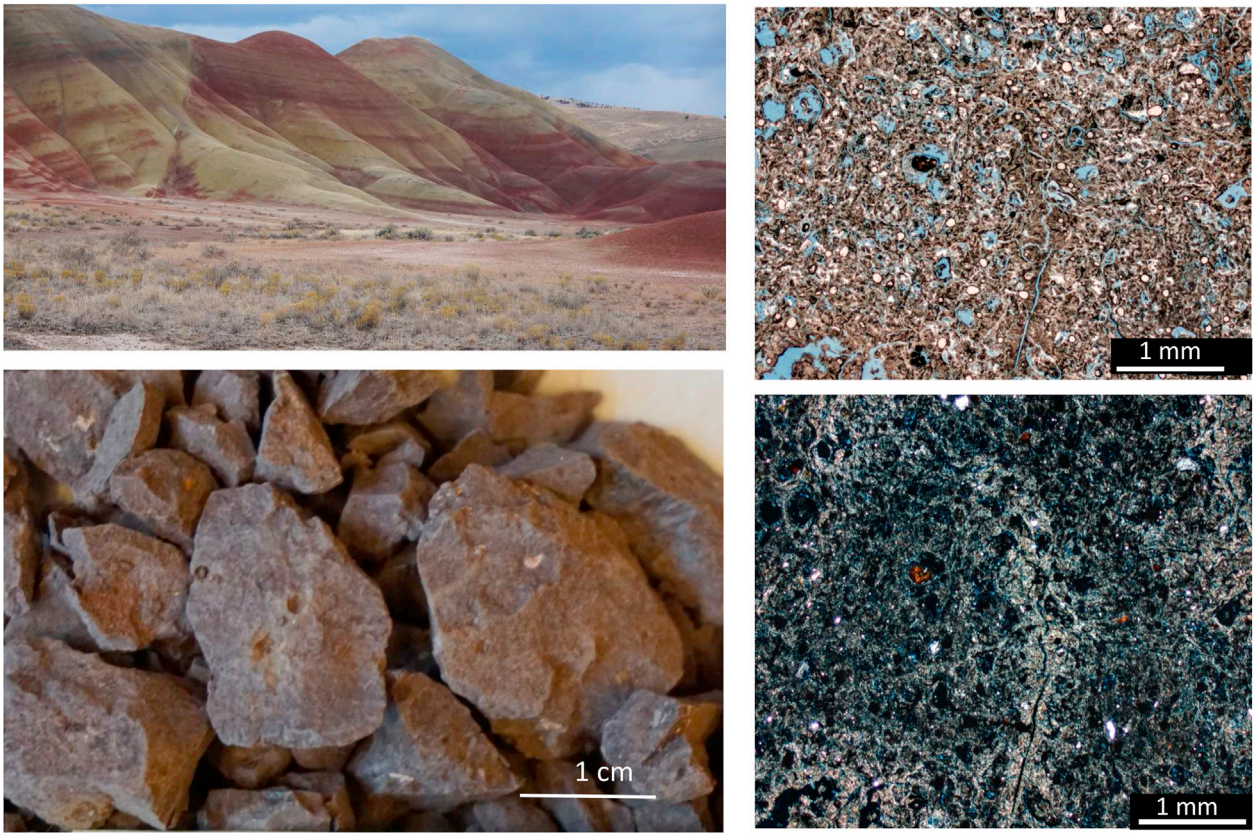

Fig. 19. Weathered tuffs, rhyolite from John Day Valley in the upper left photo. Sample JD 16–0018 (lower left) and to the right thin section photos with blue stained epoxy; upper right photo ordinary light, lower right photo crossed polarizers. Scale bar in photos.

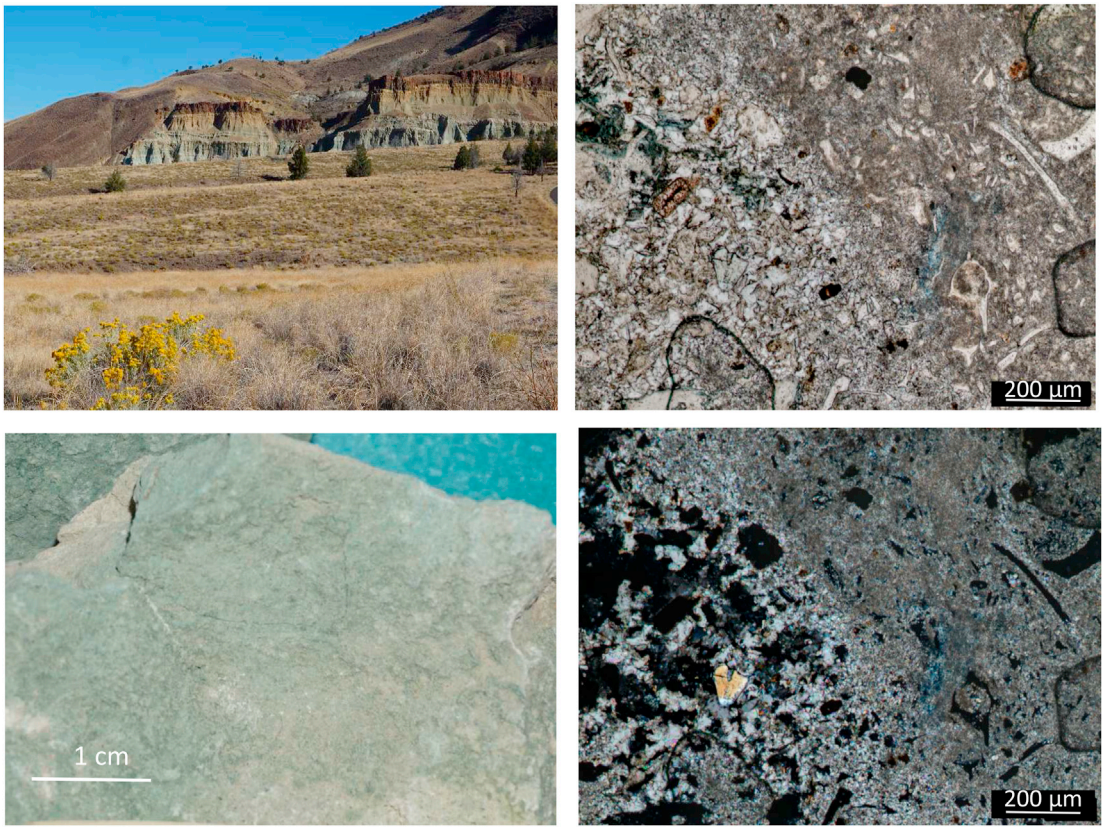

Fig. 20. Altered andesites, at Foree, John Day Valley are shown in the two left photos. Rock sample JD16-0001 in lower left photo. In the right thin section photos with blue stained epoxy; upper right photo ordinary light, lower right photo crossed polarizers. Scale bar in photos.

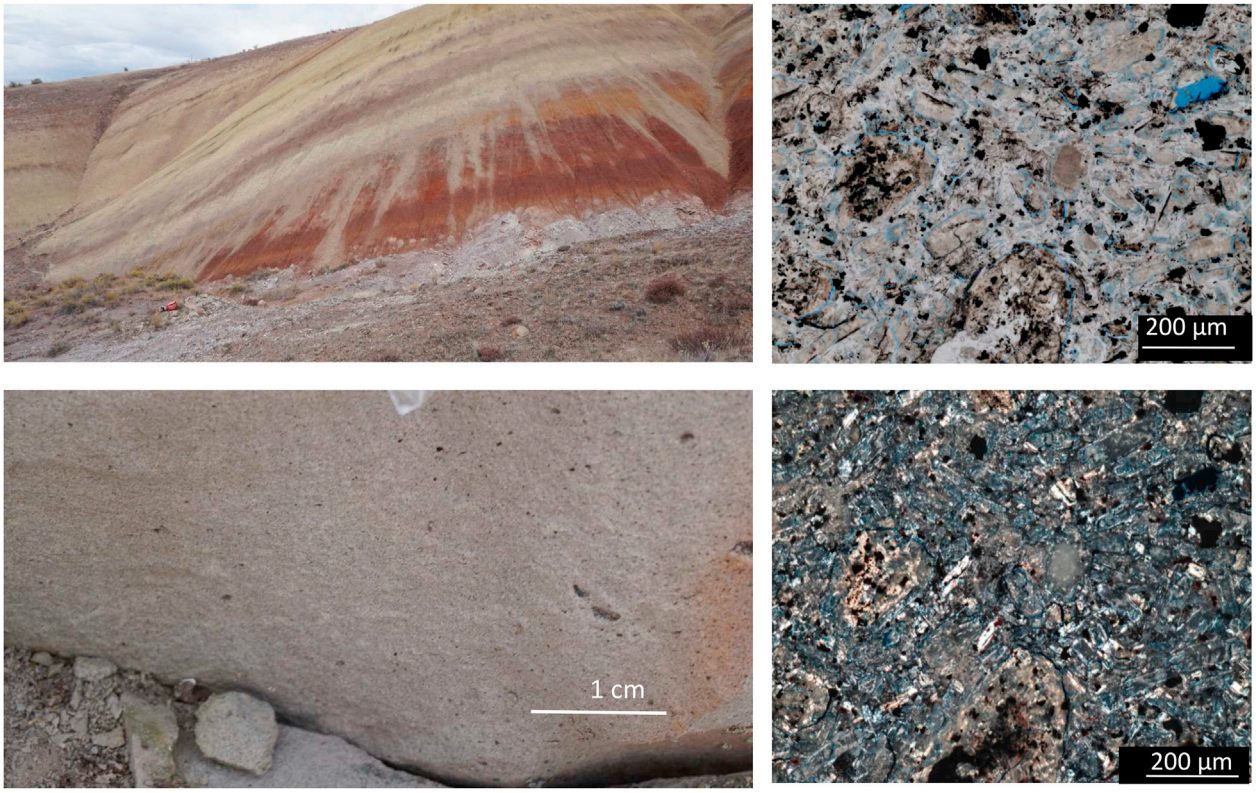

Fig. 21. Altered andesite with andisol, at John Day Valley (upper left), sample JD16-0022 (lower left). Thin section photos to the right, blue stained epoxy; upper right photo ordinary light, lower right photo crossed polarizers. Scale bar in photos.

Fig. 22. Hyaloclastite from Tamaraceite, Gran Canaria. Pencil for scale in left photo, hammer in the right photo.

Fig. 23. Altered phonolite from Tenerife, Azulejos locality. Car and road for scale.

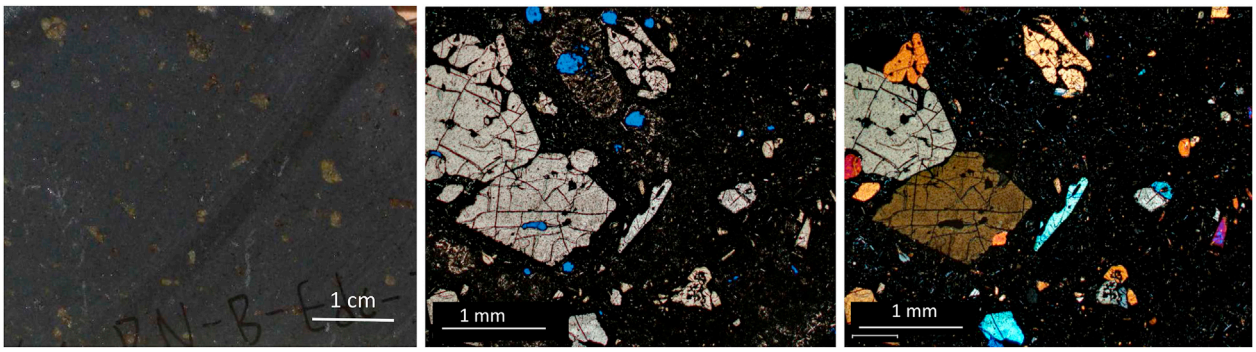

Fig. 24. Lava from Rouque Nublo, sample RN16-0001 to the left. Thin section photos with blue stained epoxy; in the middle and to the right. Middle photo ordinary light, right photo crossed polarizers. Scale bar in photos.

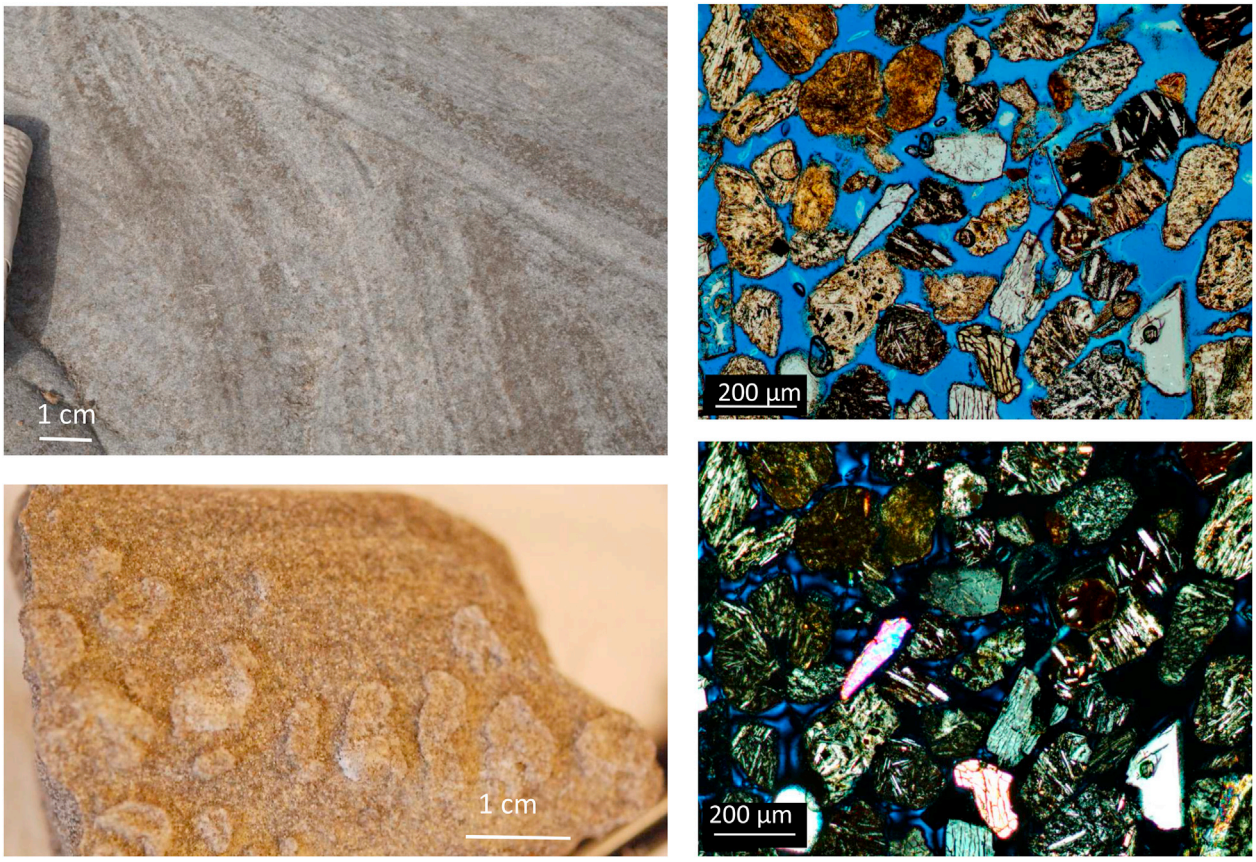

Fig. 25. Cross-bedded volcanoclastic sediments from Tenerife, Amarilla (upper left photo), the patchy cementation is shown in lower left photo, sample AMA 16-0001. Thin sections with blue stained epoxy to the right; upper photo ordinary light, lower photo crossed polarizers. Scale bar in photos.

River basalts (Figs. 17 and 18) crop out along extensive river sections. It is a succession of Miocene tholeiitic lava flows (McDougall, 1976). In the PTAL sample library, we include the Picture Gorge Basalt representing an upper mantle source (Waters, 1961; McDougall, 1976) and samples from the older, more acid andesitic, rhyolitic to dacitic dominated Eocene and Oligocene Clarno Formation, along with several paleo-weathering sections. The John Day Valley succession is rich in various Paleogene volcanic rocks and their weathering products. Fine-grained, poorly sorted, weathered tuffs (Fig. 19) are rich in larger, angular clasts of albite and potassic feldspar, with enstatite, quartz, glass clasts, and olivine in a fine matrix. The glassy fragments have partly been dissolved. Calcite and various zeolites (clinoptilolite/heulandite) precipitated and mixed layered smectite/illite clay minerals are common. The basalts of the John Day Valley contain feldspars (labradorite and anorthoclase) and augite in a very fine-grained matrix, and voids with walls coated by zeolites. The matrix is rich in feldspar and olivine, some altered to serpentine (chrysotile). These basalts occur in poorly altered and heavily altered versions, both represented in the PTAL library collection (Figs. 17–20). Some basalts are rich in hematite, smectite and mixed layered clay minerals, while remnants of plagioclase (albite, andesine, and labradorite) and orthoclase are present, together with amphibole, mica, pyroxene, ilmenite and tridymite. The fresh and weathered andesite

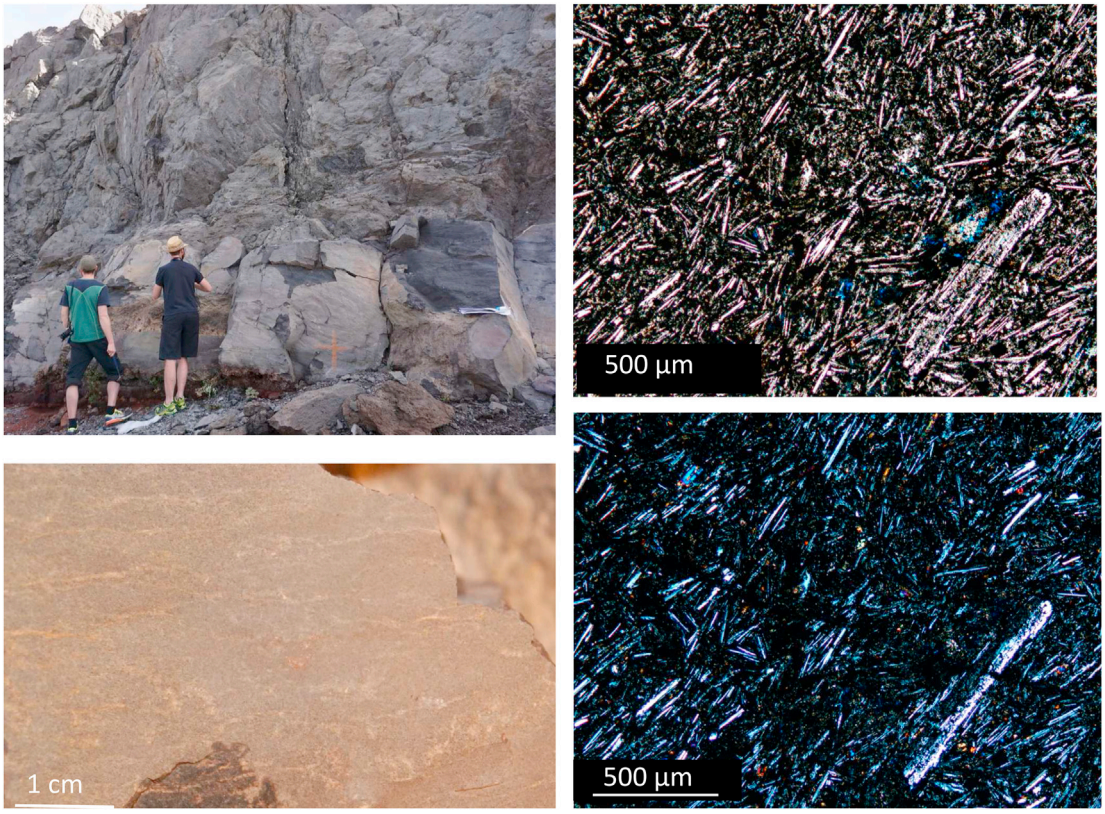

Fig. 26. Altered phonolite from Montana Reventada, Tenerife, sample MR16-0001, in the two left photos. Thin section with blue stained epoxy to the right; upper photo ordinary light, lower photo crossed polarizers. Scale bar in photos.

samples of the PTAL collection contain hematite and kaolinite in varying amounts in addition to sanidine, anorthoclase, some quartz and clay minerals (Fig. 21). The alteration in most cases is especially intense along fractures, as with the two rhyolites samples collected from the John Day Valley area. Feldspar dominates in the fine-grained matrix, commonly with hematite varnish on grains in the weathering sections. Large phenocrysts of amphibole and feldspar are common, and traces of kaolinite and chlorite are the alteration products together with hematite in the weathering sections. Quartz, sanidine, orthoclase and glass shards along with illite/smectite mixed layered clay minerals are apparent with enstatite in the matrix, as well as in vacuoles in the glassy chards. The amounts of hematite varies according to degree and type of alteration, and in the deep weathered cases lots of kaolinite and illite/smectite mixed layered clay minerals are common often together with fossil rootlet structures.

Some John Day Valley soil profiles have been sampled. In the PTAL library, very fine-grained andisols of volcanoclastic sandstones rich in celadonite, quartz, zeolites (clinoptilolite/heulandite), various plagioclases (andesite, albite) and traces of calcite and siderite were picked out (Fig. 21). Grains of quartz, feldspar, calcite, siderite and different fossils often with dark weathering coating of iron oxides are common. Angular glass shards, finely distributed zeolites and dispersed grains of pyroxene and olivine are present. Smectitic and illittic clay minerals are common in the weathered siltstones, but quartz, calcite and siderite are also present. The rock sample is well-sorted and display hematite staining (Fig. 21).

The PTAL library contains various volcanic rocks from the Canary Islands spanning lavas and volcanoclastic sandstones to different kinds hydrothermal and weathering alteration products (Troll and Carracedo, 2016). The volcanoclastic sandstones sampled are rich in volcanic rock fragments and minerals like phillipsite, sanidine, anorthosite, diopside, augite and albite. Traces of smectite and mixed layered clay minerals are also present. The sandstones are poorly sorted, composed of grains from fine silt to several mm. The grains often carry clay alteration rims, which also glue them together. The fused, poorly altered hyaloclastites are fine-grained, glass-rich volcanoclastic with dispersed larger crystals of actinolite, olivine, andesine, diopside, ilmenite, and minor amounts of chlorite and smectite. Alteration rims of possible clay minerals are common (Fig. 22). The sampled basanites commonly appear in a welded fine matrix with plagioclase (andesite), nepheline/leucite, augite, K-feldspar, olivine/forsterite, biotite, pyrite and magnetite. The olivine can be somewhat altered, but rarely became completely serpentine. The altered phonolites are rich in colorful clays at Los Azulejos (Fig. 23) and dominated by plagioclase, muscovite, augite, K-enriched large nepheline crystals, chlorite, smectite, in a brownish green ground mass. Analcime crystals are growing in the fine matrix, which is mainly composed of feldspar and brown stained, altered amphiboles.

The Roque Nublo peak of Gran Canary consists of olivine and pyroxene-rich lava (Carracedo and Troll, 2016) with olivine, biotite, nepheline and minor smectite, pyrite and zeolites. Large phenocrysts of olivine and nepheline are common and voids with secondary filling of large zeolite crystals (Fig. 24).

At Tenerife, volcanoclastic sandstones are present, e.g. along coastal outcrops in the South East (Fig. 25). The rocks contain recent halite and gypsum precipitates, in addition to augite, anorthoclase, labradorite, quartz, pyrite and phillipsite (zeolite). The sampled sandstones are very well-sorted, consisting of well-rounded grains with an average grain size of about 200 μm. The rocks contain volcanic rock fragments, often red-stained, in addition to plagioclase (andesine), K-feldspar, pyroxene, and quartz. Volcanic glass and biotite are also present, reflecting their only moderately altered composition.

The sampled phonolites from Tenerife display varying degrees of alteration, and contain muscovite, anorthoclase, sanidine, nepheline, augite, ilmenite and some quartz (Fig. 26). Large crystals of muscovite and nepheline, and some feldspar, are present in the fine feldspar matrix. In some altered phonolites, secondary unaltered analcime, phillipsite and barite may be found in a greenish-brownish fine matrix. Strongly altered

phenocrysts of plagioclase and mica can be found in the fine-grained, dark green matrix, rich in smectite. In some of the altered phonolites hematite covers large part of the rock and angular grains of quartz and feldspar, in a matrix of fine, red clay.

The Tenerife basanite is very fine-grained with elongated (0.1–0.5 mm) crystals of plagioclase, nepheline and possible leucite. In addition augite, biotite, olivine, and andesite have been detected in the very fine matrix. The samples look almost unaltered.

3.3. Altered volcanic rocks and hydrothermal deposits

Altered volcanic rocks including basalts, andesites, and basanites from Tenerife and Gran Canaria (Fig. 23), and John Day Valley (Oregon, US) (Fig. 21) have been presented above, in order to keep the presentation of fresh and related weathered formations close. The Tenerife/Gran Canaria samples have suffered additional alteration after initiation of hydrothermal activity, as recognized by their clay mineral content. It is also reflected in the vivid colours of e.g. the Los Azulejos outcrops at Tenerife, developed in various oxides on mafic and felsic rocks. Los Azulejos has been interpreted to be the results of fault controlled hydrothermal alteration formed through the lifetime of the caldera from about 200.000 years ago (Fig. 23). The Las Cañadas Caldera of Teide, Tenerife, has been active over the last few million years producing phonolitic magmas, but also more recent basaltic activity (Ancochea et al., 1990; Marti et al., 1994). Similar hydrothermal alteration products are present along the Miocene Tejeda Caldera margin at Gran Canaria where altered tuff is evident in the Fuente de Los Azulejos. A variety of hydrothermal minerals (Troll et al., 2002; Donoghue et al., 2008) developed during the last few million years (Bogaard and Schmincke, 1998). It is important to stress the difference despite a similar appearance between the John Day paleosols and Canary Island hydrothermal deposits. The alteration products of the John Day area also appear in colorful sections, rich in clay minerals and iron oxides of several varieties (Fig. 21). The colour staining there reflects thermal and chemical alteration products of permeable layers, paleosols in humid climate is the most likely explanation (Retallack et al., 2000; Sheldon, 2003; Bestland et al., 2008; Retallack, 2008). The different sedimentary and tuffaceous formations are highly weathered and were possibly later diagenetically altered into fantastic shapes and colours (Figs. 19 and 21).

The cordillera where Jaroso Ravine is located (Figs. 1, 27 and 28) in a tectonic active Paleocene to Pliocene zone rich in economically important minerals, partly products of hydrothermal activity (Arribas and Tosdal, 1994; Rull et al., 2005). Within this region, the Jaroso hydrothermal system (JHS) has been identified as a good analogue to the hydrothermal processes that occurred in early Mars (Martinez Frias et al., 2004). Linked to Miocene calc-alkaline and shoshonitic volcanism, JHS provides clear geological and mineralogical evidence of interactions between tectonic, volcanic, evaporitic and hydrothermal processes. As described in previous studies, JHS presents heterogeneous assemblages of sulphate mineral (jarosite, copiapite and rozenite, among others) and iron oxides (goethite and hematite). This mineral association is very similar to those detected at Mars by the Opportunity rover at Meridiani Planum (Klingelhöfer et al., 2004).

The PTAL sample analysed represents a fracture-filling in mica schists, and is rich in jarosite, other sulphates, feldspar (orthoclase) and carbonates (Martinez-Frias et al., 2004, 2007) (Fig. 28). In detail, sample JA08-501 was collected from a sulphate deposit and it is mainly composed of jarosite. Sample JA08-502 present a higher mineralogical variety, where iron-based oxides (ilmenite and goethite) are found together with putative hydrothermal products (barite), among others. Sample JA08-503 was collected from a shale-based soil and displays a complex mineralogy, including quartz, illite, goethite and iron oxides, kaolinite and potassic

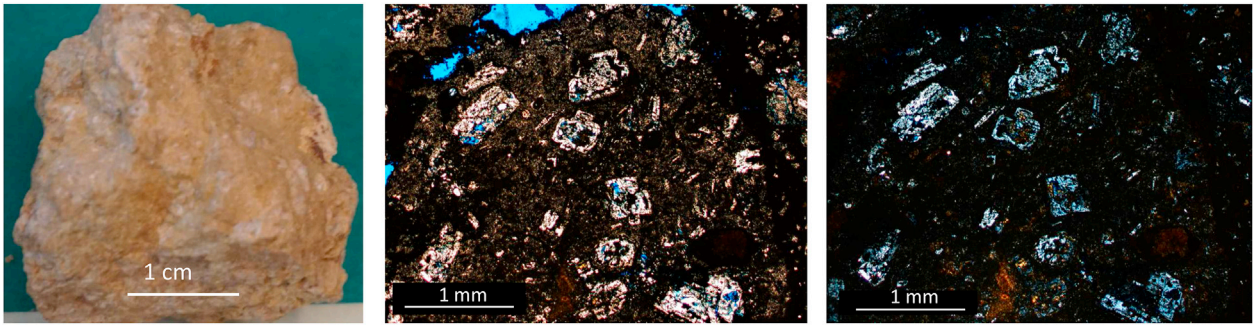

Fig. 27. To the left a photo of sample JA08-501 from Jaroso Ravine. To the right thin section photos with blue stained epoxy; the middle photo ordinary light, the right photo crossed polarizers. Scale bar in photos.

Fig. 28. The entrance of the Jaroso Ravine is shown to the right, while sampling of the Jaroso Ravine sample is displayed in the left photo.

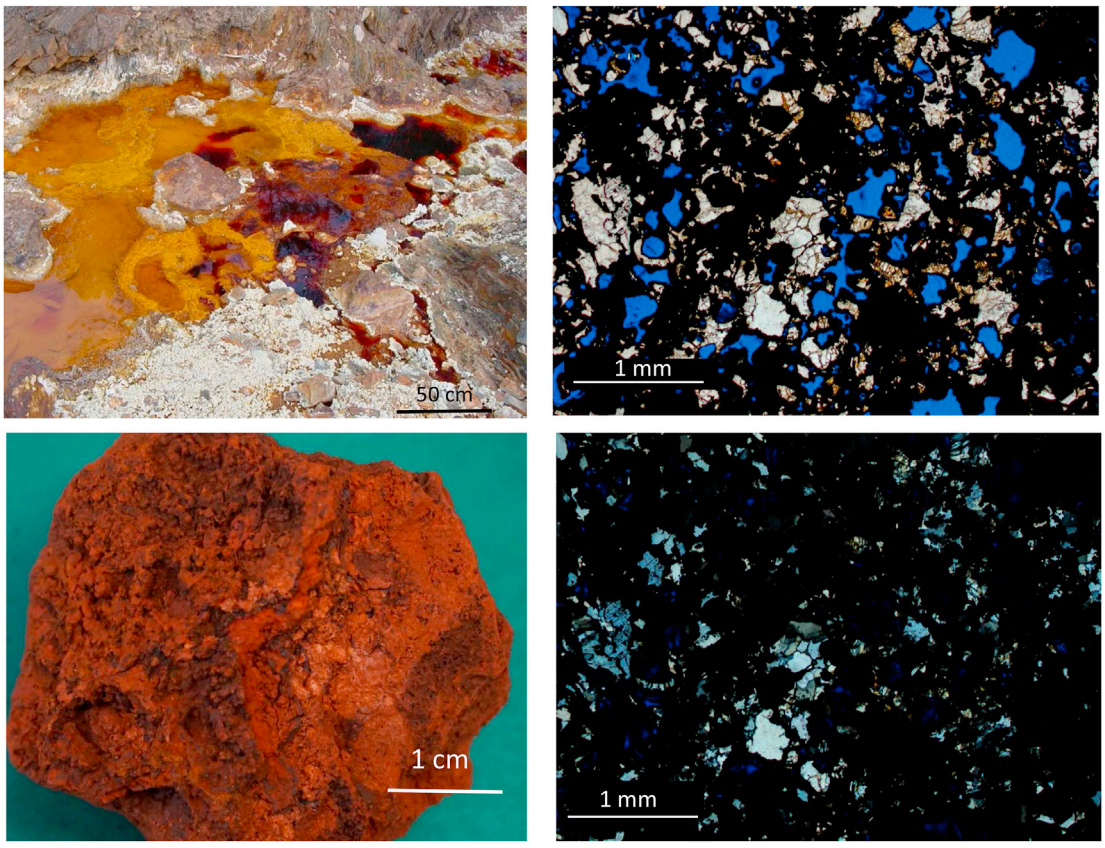

Fig. 29. Rio Tinto field appearance (upper left) and sample RT03-501 (lower left). To the right thin sections with blue stained epoxy; upper photo ordinary light, lower photo crossed polarizers. Scale bar in photos.

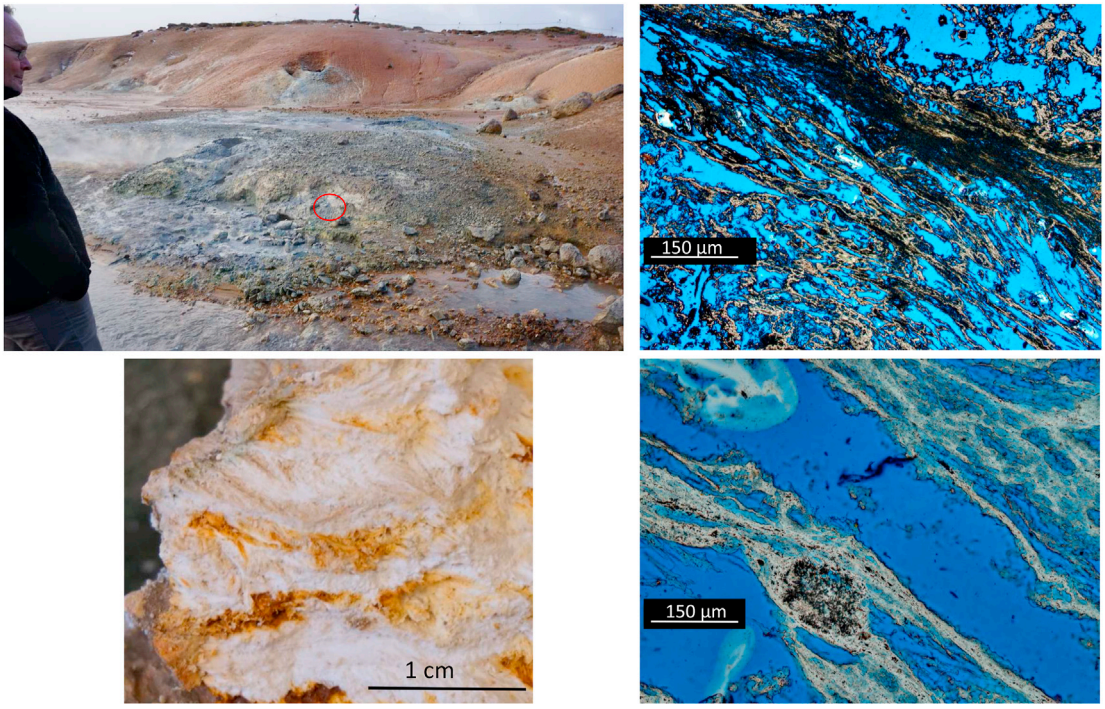

Fig. 30. Seltun at Reykjanes Peninsula (upper left) and sample IS16-0010 (lower left), solfatara precipitate, amorphous material. To the right thin section photos, blue stained epoxy; upper photo ordinary light, lower photo crossed polarizers. Sample at red circle. Scale bar in photos.

feldspar, hematite, calcite, anatase carbon and barite.

Iron oxide precipitates from Rio Tinto are also included in the PTAL library (Figs. 1 and 29).

Rio Tinto is a 100 km long river located at the Iberian Pyrite Belt,

which is considered one of the largest sulfidic deposits in the world (mostly iron and copper sulphides) (Boulter, 1993; Hudson-Edwards et al., 1999; Amils et al., 2007, 2014). In this site, exhalative ores can be also found in brine pools or as veins. Partially as a consequence of mining activities, the red waters of the river are characterized by highly acidic values (mean pH below 2.5) and a remarkable concentration of heavy metals (mostly Fe, Cu, Zn and As). The Rio Tinto sulphide deposits of southern Spain are hosted in highly tectonised volcanic rocks, formed during Devonian to Carboniferous tectonics. One of the Rio Tinto samples is a pegmatite rich in quartz, hematite, zoisite and enstatite. A section of the sample appears like quartzite, with several pits, hematite and iron oxide filling most of the porous structure. Other parts of the sample is clayey with sulphates, but also pyrite and other opaque grains (Fig. 29). The second analogue sampled in this region correspond to an extremely weathered rock presenting iron oxides and quartz as the main mineralogical phases. A third sample was collected from an area presenting sulphide-based deposits (mainly pyrite).

At Seltun (Figs. 1, 11 and 30) on Iceland, selected hydrothermal formations were sampled. The deposits consist of amorphous material, characterized by very poor diffractograms, but some large crystals of pyroxene and various feldspars are apparent. The major part of this glassy sediment display a fine-grained, brownish Fe-rich matrix with possible Zn-sulphides and pyrite present. The XRD patterns are difficult to interpret because of the amorphous glassy and amorphous Fe-oxide rich phases.

As discussed above and illustrated by the John Day sections and Los Azulejos locations of Tenerife and Gran Canaria, the results of hydrothermal activity may often be difficult to separate from, e.g. the alteration due to weathering. Hydrothermal activity commonly appears in volcanic terrain, in tectonic active areas, but also in impact crater settings. In this library, we have hydrothermal samples from Iceland, Canary Islands, John Day Valley, Leka, Rio Tinto and Jaroso Ravine, which all likely suffered additional degrees of post-depositional alteration.

3.4. Plutonic igneous rocks

A small selection of magmatic rocks are present in the PTAL library collection (Fig. 1 and Table 1): lhzerzolites, pyroxenites, dunites from Ullernåsen in Oslo, Norway (Dons, 1952; Neumann et al., 1985) (Fig. 31), the Oslo Rift, i.e. Brattåsen along the Oslofjord, Norway (Figs. 32 and 33), and the island of Leka, Mid-Norway (Figs. 34–36). The gabbroic samples of the Oslo rift area have been dated to between 245 and 304 million years (Permian), and the different gabbros are overall concentrically arranged (Neumann et al., 1985). The Ullernåsen area is located in a heavy populated region within the town of Oslo, so the olivine-clinopyroxene rocks are exposed to and modified by human activities such as intense gardening, in addition to metamorphism and weathering. Consequently the bulk rock from Ullernåsen display reduced amounts of olivine and plagioclase, and pyroxene somewhat altered to biotite, chlorite, Fe-Ti-oxides and sericite (Dons, 1952; Neumann et al., 1985) (Fig. 31). The Ullernåsen sample in addition contains minor amounts of cordierite, hematite and magnetite, no serpentinite was found.

In Brattåsen (location Viksberget in Neumann et al., 1985), the complex gabbroic rocks are rich in diopside, actinolite, plagioclase and biotite, and chlorite is also present. The lithologies show only modest alteration, such as minor parts of the plagioclase to sericite and pyroxene parts to biotite (Figs. 32 and 33). Some grains are fractured with minor internal alteration and carbonate filled fractures.

The late Cambrian Leka Ophiolite Complex (LOC), which most likely represents a supra-subduction zone, is today part of the so-called Upper/Uppermost Allochthon (Furnes et al., 1988). The complex is rich in

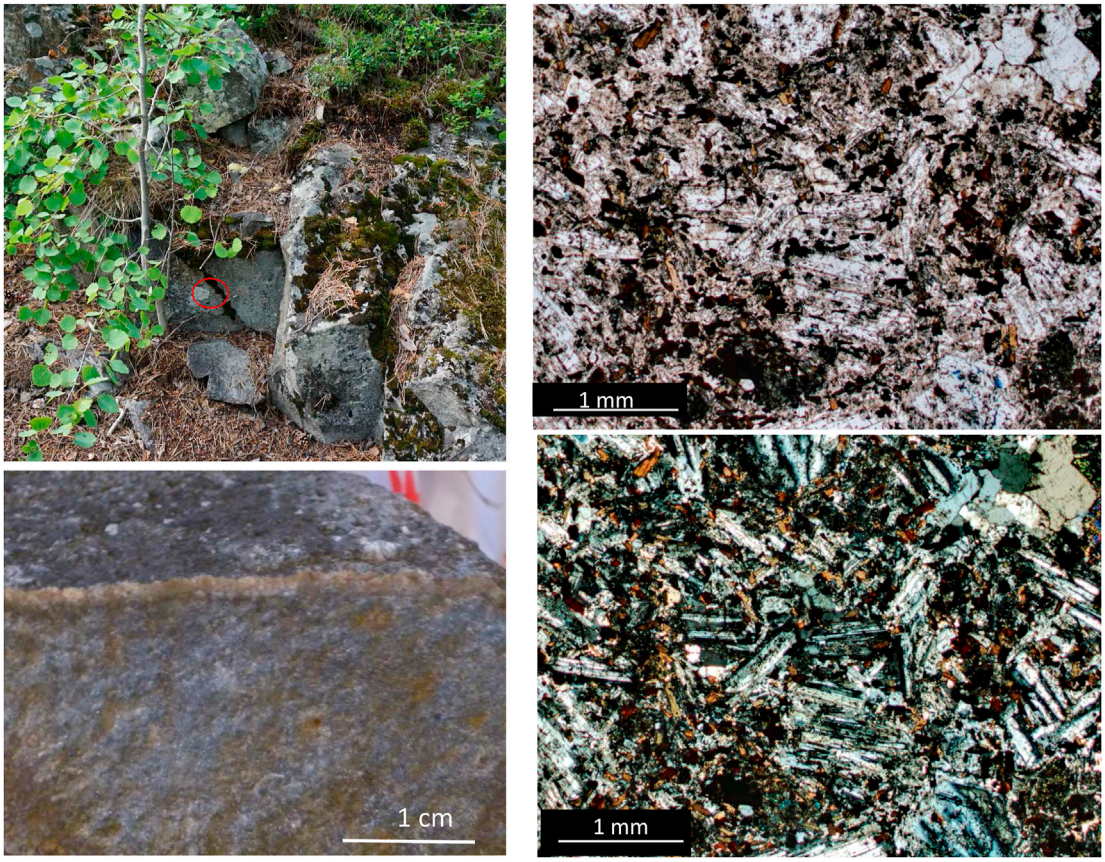

Fig. 31. Field appearance (in a local private garden) and the rock sample UL16-0001 (gabbro) at Ullernåsen, Oslo. To the right thin section photos, blue stained epoxy; upper photo ordinary light, lower photo crossed polarizers. Sample at red circle. Scale bar in photos.

Fig. 32. Brattåsen location at the rim of the Oslo rift, the Oslo Fjord in the background, sample BR 16-0001 with hammer in front. Sampled at hammer location. To the right detail photo of sample BR16-0001, a gabbro rich in pyroxene.

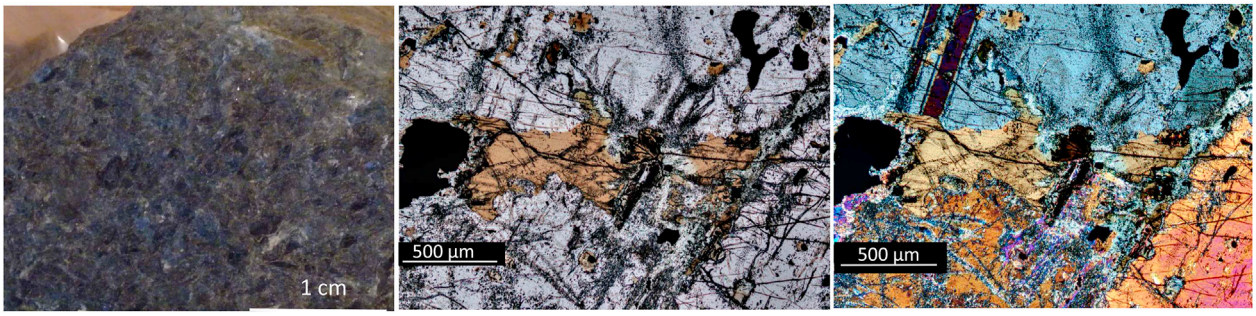

Fig. 33. Brattåsen sample BR 16-0001 (to the left), in the middle and to the right thin section photos, blue stained epoxy. In the middle photo in ordinary light and in the right photo with crossed polarizers. Scale bar in photos.

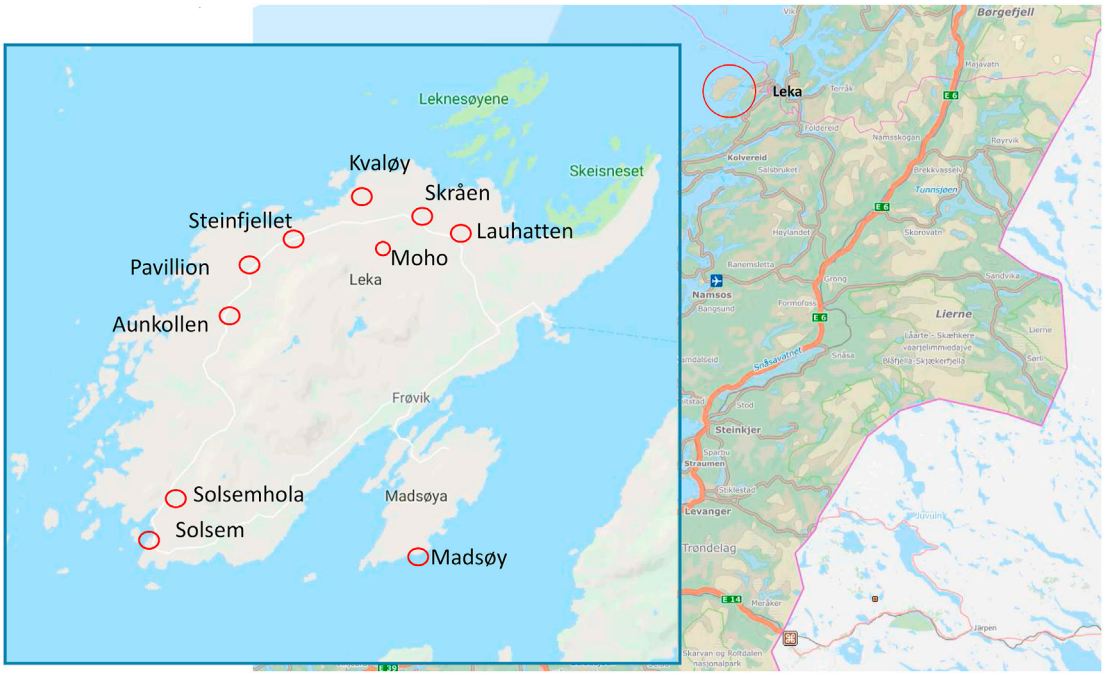

Fig. 34. Map of the Leka island in Mid-Norway. Sample sites are marked by red circles. Scale: The length of Leka Island is 12 km.

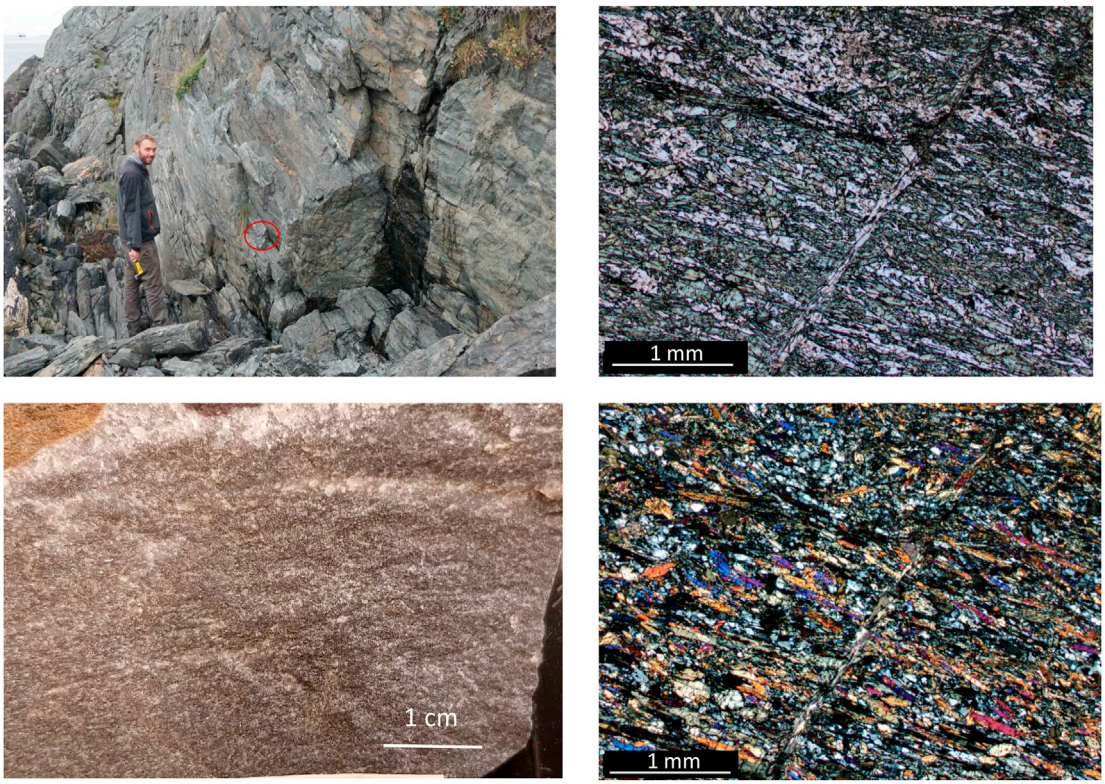

Fig. 35. The pillow lavas of tholeiitic composition at Madsøy, Leka (upper left)(see map in Fig. 34). Sample LE16-0013 (lower left). To the right thin section photos with blue stained epoxy; upper photo ordinary light, lower photo crossed polarizers. Sample at red circle. Scale bar in photos.

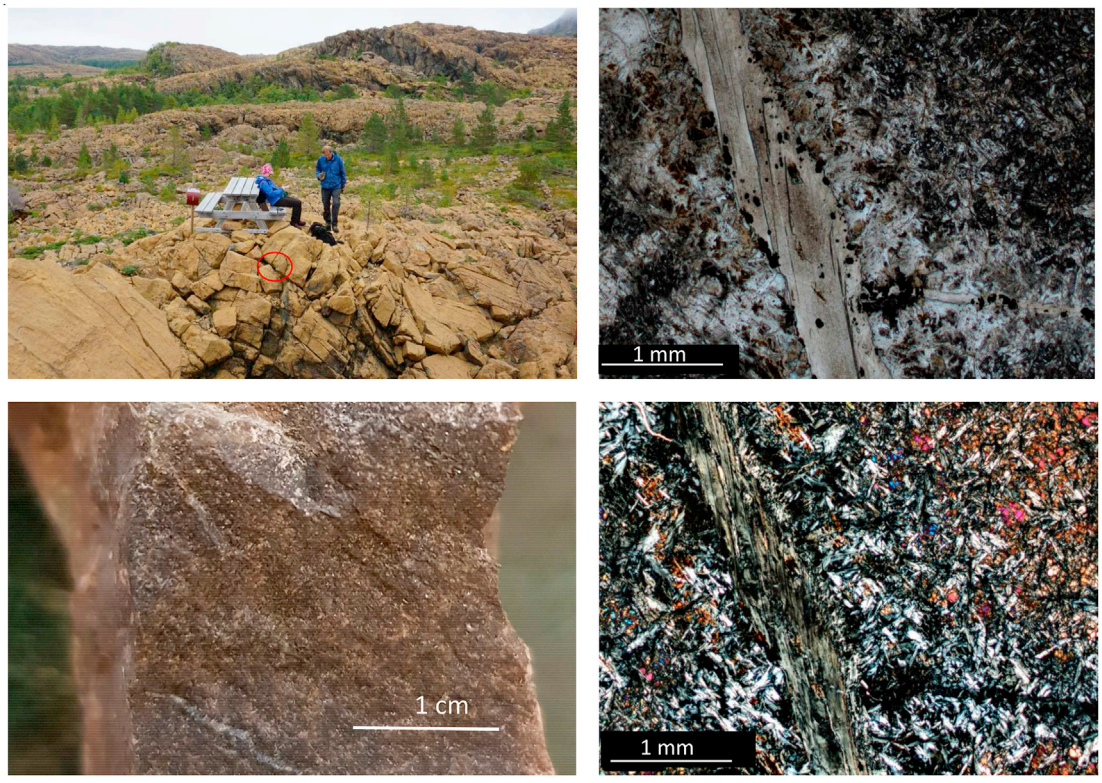

Fig. 36. The so-called Moho-tourist site at central Leka (see map in Fig. 34), to the upper left. Sample LE16-00016 of Harzburgite from the Moho-site (lower left). Thin section photos with blue stained epoxy to the right; upper photo ordinary light, lower photo crossed polarizers. Sample at red circle. Scale bar in photos.

gabbros, harzburgites and various layered ultramafic rocks. It contains partly to completely serpentinised and carbonated peridotites (Bjerga et al., 2015) (Figs. 35 and 36). Pillow lavas are capping the ultramafic rocks and have composition varying from island arc tholeiites to MORB type lavas, possibly representing late spreading stages of the LOC. The PTAL collection of rocks from Leka is rich, spanning harzburgites, lherzolites, dunites, tholeiites, and serpentine conglomerates (Figs. 34–36). The Leka collection has similarities to the Nili Fossae region geology on Mars (Brown et al., 2010; Ehlmann et al., 2009, 2011).

The harzburgite of Leka is heavily altered, consisting of serpentine with small amounts of olivine, pyroxene and amphibole. Serpentinisation of olivine is almost complete in some of the samples, while the pyroxenes and amphiboles are less altered. Magnetite is present and most likely formed during the serpentinisation of the olivine. The dunite was originally dominated by forsterite and augite, now serpentinised to antigorite, especially well-developed replacement along fractures. Magnetite may also be present. The present appearance of Mg-enriched chlorites and epidote reflects greenschist facies metamorphism. The more gabbroic layers are rich in pyroxene (diopside) and amphibole (hornblende). They display some pyroxene alteration to chlorite and epidote along cleavage planes and chlorite are present in voids. Some layers rich in chromite occur. The uppermost parts of the Leka succession is dominated by pillow lava (Fig. 35), with hornblende, plagioclase, some pyroxene, olivine and chlorite. Calcite is present in greenschists, representing metamorphic greenschist facies, in part replacing the original minerals (clinopyroxene, plagioclase, olivine and amphibole). Calcite precipitates appear in original pore space. In the Leka sections there are also serpentine conglomerates, in a grain-supported texture consisting of rounded to angular grains, a mix of mainly harzburgite and dunite clasts.

4. Alteration experiments

Alteration experiments complement the analogues samples collection in order to understand how environmental factors affect the degrees of alteration. The goal is to relate the experiment products to the occurrences of particular alteration products at the martian surface. It should be noted that altered martian lithologies probably will be best represented by the products of the laboratory experiments, since no organisms interfered, which most likely is the case for surface alterations in our terrestrial samples. We found even in very fresh, quarried, recently-formed volcanic rocks from Iceland, biological influence. Consequently, it will be of interest to compare the laboratory alteration products with those of the PTAL collection. Since the laboratory experiments are all hydrothermal, the best comparison is between these and alteration features in the collected impact rocks and hydrothermal deposits. Nevertheless, it is also of interest to understand how some of the phyllosilicates were formed from both low-temperature Earth-like conditions, as well as during hydrothermal alteration.

The samples used in the experiments were selected from the PTAL collection, based on a minimal content of alteration phases and on capability to undergo reaction fast enough (laboratory-scale as opposed to natural conditions-scale) to be studied in laboratory. The fresh and young tholeiitic glass from Stapafell (Iceland) was used in several of the experiments due to the fast reaction kinetics of glass compared to crystalline materials of comparable chemical composition. The reaction rates are, however, still slow at ambient conditions, and experiments were consequently executed with finely crushed materials and most were reacted at hydrothermal conditions ($T > 100\ ^{\circ}C$). The experiments therefore most closely resemble martian alteration associated with post-impact hydrothermal activities. It should, however, be noted that several of the alteration phases may have been formed at low temperatures, and the hydrothermal conditions merely speed up the alteration process.

A first series of experiments was performed to study the alteration of impact related material (Declercq et al., 2009; Hellevang et al., 2013; Sætre et al., 2018). The alteration experiments of tholeiitic material revealed zeolites as common products, but this mineral group has rarely been described from Mars (Carter et al., 2013). It also suggests that post-impact hydrothermal alteration of ejecta deposits can play a significant role. Finally, it allowed to set the conditions needed to form most of the alteration mineral associations seen on Mars. Because it became possible that the presence of zeolites on Mars may be underestimated (Sætre et al., 2018), another series of experiments focused on competition of formation of clays, zeolite and carbonates (Viennet et al., 2017). It concludes that if zeolites are not present on Mars, it could reflect the acidic pH of the solution. Finally, other experiments focused on deciphering the conditions of alteration at probable ESA's Rosalind Franklin Rover landing site (ExoMars). First, on weathering profiles, that can serve as proxy to the early Mars atmosphere (Viennet et al., 2019b) and then on possible pathways of alteration for vermiculitisation in martian conditions (Krzesińska et al., 2019, 2021).

5. Implications

The PTAL library is a broad lithological collection of terrestrial samples, which will act as good analogues for martian rocks, towards a goal of getting optimal quality remote and in-situ analyses with the equivalent instruments on board of the Mars2020 and the ExoMars rovers. Presently most of the comparable analyses are based on comparison with standards of ultra clean minerals, thereby lacking the effects of mineral-mineral interferences, grain-size dependences and natural mineral mixture background in the analysis. The PTAL collection offers an important contribution in this respect. The PTAL rocks and samples are open to all researchers, and the collection may even in some cases work as an inspiration for trying out new analytical methods.

It is difficult to get an optimal sample collection of martian analogues since most terrestrial rocks and sediments have been weathered and altered by both geochemical processes and some sort of biogenic activity; we have not been able to collect totally pristine (not weathered/altered) surface samples on Earth. Even the most recently formed Icelandic volcanic rocks sampled in an active quarry of very young formations carry indications of life. Organic overprint as part of the so-called deep biosphere has been found in deep granite fractures 740 m below the surface in Laxemar, Sweden (Drake et al., 2017). In the present experiments, such geochemical and biological interference may create analytical problems, but the sample collection was the best we could get also in that respect. In spite of these biological contamination difficulties, it should be possible to sort out analytical problems related to, e.g. matrix and background complications, grain-size dependence, and mineral-mineral interferences.

Our collection does also provide for the first time a systematic comparison of the results of the different analytical methods applied on the very same samples. Thereby, it is possible that the PTAL library also will aid in methodological improvements, e.g. better recognition of quartz and feldspar by near infrared spectroscopy analyses. Presently results of traditional analysis optical studies, XRD, NIR, RAMAN and LIBS are included in the PTAL library. Since the samples will be available, additional analyses such as e.g. isotope studies could be added to better elaborate on sample origin and presampling history. The ultimate goal of the PTAL library is to support better analysis both quantitatively and qualitatively, overcoming the challenge of comparison with pure mineral analogues. Maybe with the help of the PTAL approach, future detections of new phases, e.g. feldspar species, zeolites and phosphates, may become possible.

Comparing the information of the geological sample context on Earth, may aid the interpretation of mineral formation on Mars. However, such comparison is challenging as many processes on Earth related to plate tectonics, are bio-mediated or occur under different atmospheric compositions. The organization of the PTAL library, its curating and sample handling has not been discussed in great detail, but is a point of great importance giving scientist access to PTAL samples and data. It is likewise a financial question having somebody updating, serving and curating the collection, along with a scientific/administrative group

taking the necessary and correct decisions on who should get samples and which new samples may be collected.

Author statements

HD led the preparation of the manuscript, performed and coordinated field campaigns. HD, HH, AK, CS, JCV, DR, FR collected samples, HD, HH, AK, JCV, BB, DL, MV, AC characterised the samples with the methods described in the manuscript, BB, AK, DL, FP, FR, SCW described the martian context. HD, FP, FR, SCW coordinated the different work package activities, SCW developed, coordinated the research and project overall. ALL authors discussed the results and contributed equally to writing the manuscript.

Declaration of competing interest

The authors declare that they have no known competing financial interests or personal relationships that could have appeared to influence the work reported in this paper.

Acknowledgements

This project is a collaborative work between the University of Oslo (Norway), University of Paris-Saclay and University of Toulouse (France), as well as the University of Valladolid (Spain) under the EU Horizon 2020 Space programme call H2020-COMPET-2015-Grant Agreement no 687302. Updated information on the access and release of data we will published on www.ptal.eu.

AMK, BB, JCV, HD, CS and SCW were additionally supported by the Research Council of Norway through its Centres of Excellence funding scheme, project number 223272 (CEED).

We appreciated knowledge, field- and laboratory support, and sample supply and therefore thank: Håkon Austrheim, John Carter, Alvaro Crosta, J. Wright Horton Jr., Dougal Jerram, Jon Jonsson, Bjørn Tore Larsen, Thanusha Naidoo, Else Ragnhild Neumann, Francisco Jose Perez Torrado, Greg Retallack, Lucie Riu, Akthavan Salahalldin, Valentin Troll, Reidar Trønnes. We would also like to thank editor in chief Angelo Pio Rossi, reviewer L. Mandon and one anonymous reviewer for valuable comments.

References

Allen, C.C., Gooding, J.L., Keil, K., 1982. Hydrothermally altered impact melt rock and breccia: contributions to the soil of Mars. J. Geophys. Res. , Solid Earth B12, 10083–10101. https://doi.org/10.1029/jB087iB12p10083.

Amils, R., Toril, E.G., Remolar, D.F., Aguilera, F.G., Rodríguez, A.N., Malki, M., García-Moyano, A., Fairén, A.G., la Fuente, V., Sanz, J.L., 2007. Extreme environments as Mars terrestrial analogs: the Rio Tinto case. Planet. Space Sci. 55, 370–381.

Amils, R., Remolar, D.F., the IPBSL team, 2014. Río Tinto: a geochemical and mineralogical terrestrial analogue of Mars. Life 4, 511–534.

C. Ancochea, E., Fustere, J.M., Ibarrola, E., Cendrero, A., Coello, J., Hernan, F., Cantagrei, J.M., Jamond, C., 1990. Volcanic evolution of the island of Tenerife (Canary Islands) in the light of new K-Ar data J. Volcanol. Geoth. Res. 44, 23–249.

Armstrong, R.L., 1978. K-Ar dating: late Cenozoic McMurdo volcanic group and Dry Valley glacial history, Victoria Land, Antactica. N. Z. J. Geol. Geophys. 21, 685–698.

Arribas, A., Tosdal, R.M., 1994. Isotope composition of Pb in Orde deposits of the betic cordillera, Spain: origin and relationship to other European deposits. Econ. Geol. 89, 1074–1093.

Barlow, N.G., 1988. Crater size-frequency distributions and a revised Martian relative chronology. Icarus 75, 285–305. https://doi.org/10.1016/0019-1035(88)90006-1.

Belkin, H.E., Horton Jr., J.W., 2009. Silicate Glasses and Sulfide Melts in the ICDP-USGS Eyreville B Core, Chesapeake Bay Impact Structure, vol. 458. Geological Society of America, Special Paper, Virginia, USA, pp. 447–468.

Bestland, E.A., Forbes, M.S., Krull, E.S., Retallack, G.J., Fremd, T., 2008. Stratigraphy, paleopedology, and geochemistry of the Middle Miocene Mascall Formation (type area, central Oregon, USA). PaleoBios 28, 41–61.

Bibring, J.-P., Langevin, Y., Gendrin, A., Gondet, B., Poulet, F., Berthé, M., Soufflot, A., Arvidson, R., Mangold, N., Mustard, J., Drossart, P., 2005. Mars surface diversity as revealed by the OMEGA/Mars express observations. Science 307 (5715), 1576–1581.

Bibring, J.-P., Hamm, V., Pilorget, C., Vago, J.L., the MicrOmega Team, 2017. The MicrOmega investigation onboard ExoMars. Astrobiology 17, 621–626.

Bjerga, A., Konopasek, J., Pedersen, R.B., 2015. Talc-carbonate alteration of ultramafic rocks wihin the Leka Ophiolite Complex, Central Norway. Lithos 227, 21–36.

Bogaard, P., Schmincke, H.U., 1998. Chronostratigraphy of gran Canaria. In: Weaver, P.P.E., Schmincke, H.U., Firth, J.V., Duffield, W. (Eds.), Proceedings of the Ocean Drilling Program Scientific Results, vol. 157, pp. 127–140.

Borg, L.E., Connelly, J.N., Nyquist, L.E., Wiesmann, H., Reese, Y., 1999. The age of the carbonates in martian meteorite ALH84001. Science 286, 90–94.

Boulter, C.A., 1993. Comparison of Rio Tinto, Spain and Guaymas Basin, Gulf of California: an explanation of a supergiant massive sulfide deposit in an ancient sill-sediment complex. Geology 21, 801–804.

Brearley, A.J., 1998. Magnetite in ALH 84001: Product of the Decomposition of Ferroan Carbonate. 29. Lunar and Planetary Science Conference, 16-20 March. Abstract 1451.

Bridges, J.C., Grady, M.M., 1999. A halite-siderite-anhydrite-chlorapatite assemblage in Nakhla: mineralogical evidene for evaporates on Mars. Meteoritics Planet Sci. 34, 407–415.

Brown, A.J., Hook, S.J., Baldridge, A.M., Crowley, J.K., Bridges, N.T., Thomson, B.J., Marion, G.M., de Souza Filho, C.R., Bishop, J., 2010. Hydrothermal formation of clay-carbonate alteration assemblages in the Nili Fossae region of Mars. Earth Planet Sci. Lett. 297, 174–182.

Bultel, B., Viennet, J.-C., Poulet, F., Carter, J., Werner, S.C., 2019. Detection of carbonates in martian weathering profiles. J. Geophys. Res.: Planets 124, 989–1007. https://doi.org/10.1029/2018JE005845.

Cannon, K.M., Mustard, J.F., 2015. Preserved glass-rich impactites on Mars. Geology 43, 635–638.

Carracedo, J.C., Troll, V.R., 2016. The Geology of Canary Islands. Libro, p. 621.

Carter, J., 2012. Étude des minéraux hydratés à la surface de Mars par les imageurs hyperspectraux OMEGA/MEx et CRISM/MRO. PhD thesis defended 17/10/2012 at Paris 11 University.

Carter, J., Poulet, F., 2013. Ancient plutonic processes on Mars inferred from the detection of possible anorthositic terrains. Nat. Geosci. 6, 1008–1012.

Carter, J., Poulet, F., Bibring, J.-P., Mangold, N., Murchie, S.M., 2013. Hydrous minerals on Mars as seen by the CRISM and OMEGA imaging spectrometers: updated global view. J. Geophys. Res. 118, 831–858.

Carter, J., Loizeau, D., Mangold, N., Poulet, F., Bibring, J.-P., 2015. Widespread surface weathering on early Mars: a case for a warmer and wetter climate. Icarus 248, 373–382.

Changela, H.G., Bridges, J.C., 2010. Alteration assemblages in the nakhlites: variation with depth on Mars. Meteoritics Planet Sci. 45, 1847–1867. https://doi.org/10.1111/j.1945-5100.2010.01123.x.

Chipera, S.J., Bish, D.L., 2013. Fitting full X-ray diffraction patterns for quantitative analysis: a method for readily quantifying crystalline and disordered phases. Adv. Mater. Phys. Chem. 3, 47–53.

Clark, R.N., King, T.V.V., Klejwa, M., Swayze, G.A., Vergo, N., 1990. High spectral resolution reflectance spectroscopy of minerals. J. Geophys. Res. 95, 12653.

Clegg, S.M., Wiens, R.C., Anderson, R., Fornie, O., Frydenvang, J., Lasue, J., Cousin, A., Paayre, V., Boucher, T., Darby Dyar, M., McLennan, S.M., Morris, R.V., Graff, T.V., Mertzmann, S.A., Ehlmann, B.L., Belgacem, I., Newsom, H., Clack, B., Maurice, S., 2017. Recalibration of the Mars Science laboratory ChemCam instrument with an expanded geochemical database. Spectrochim. Acta B Atom Spectrosc. 129, 64–85.

Corrigan, C.M., Harvey, R.P., 2004. Multi-generational carbonate assemblages in maertian meteorite Allan Hills 84001: implications for nucleation, growth and alteration. Meteoritics Planet Sci. 39, 17–30.

Crosta, A., Koeberl, C., Furuie, R.A., Kazzuo-Vieira, C., 2010. The first description and confirmation of the Vista Alegre impact structure in the Parana flood basalts of southern Brazil. Meteoritics Planet Sci. 45, 181–194.

Crosta, A., Kazzuo-Vieira, C., Pitarello, L., Koeberl, C., Kenkmann, T., 2012. Geology and impact features of Vargeao Dome, southern Brazil. Meteoritics Planet Sci. 47, 51–71.

Declercq, J., Dypvik, H., Aagaard, P., Jahren, J., Ferrell Jr., R.E., Horton Jr., J.W., 2009. Experimental alteration of artificial and natural impact melt ro k from Chespeake Bay impact structure. Geol. Soc. Am. 458, 5559–5569. Special Paper.

Dehouck, E., Chevrier, V., Gaudin, A., Magnold, N., Mathe, P.E., Rochette, P., 2012. Evaluating the role of sulfide-weathering in the formation of sulfates and carbonates on Mars. Geochim. Cosmochim. Acta 90, 47–63.

Donoghue, E., Troll, V.R., Harris, C., O'Halloran, A., Walter, T.R., Torrado, F.J.P., 2008. Low –temperature hydrothermal alteration of intra-caldera tuffs, Miocene Tejeda caldera, gran Canaria, canary islands. J. Volcanol. Geoth. Res. 176, 551–564.

Dons, J.A., 1952. Studies of the igneous rock complex of the Oslo Region.XI. Compound volcanic neck, igneous dykes and fault zone in the Ullern-Husebyåsen area. Det Norske Vitenskaps Akademi Skrifter, Oslo, I. Mat.Nat.Klasse 2, 96pp, 1952.

Drake, H., Ivarsson, M., Bengtson, S., Heim, C., Siljestrøm, S., Whitehouse, M.J., Broman, C., Belivanova, V., Åstrøm, M.E., 2017. Anaerobic consortia of fungi and sulfate reducing bacteria in deep granite fractures. Nat. Commun. 8, 1–9.

Dreibus, G., Wänke, H., 1985. Mars, a volatile-rich planet. Metoritic. Planet. Sci. 20, 367–381.

Dypvik, H., Gohn, G.S., Edwards, L.E., Horton, J.W., Powars, D.S., Litwin, R.J., 2018. Chesapeake Bay Impact Structure – Development of Brim Sedimentation in a Multilayered Marine Target, vol. 537. Geological Society of America, Special Paper, p. 68.

Edwards, P.H., Bridges, J.C., Wiens, R., Anderson, R., Dyar, D., Fisk, M., Thompson, L., Gasda, P., Filiberto, J., Schwenzer, S.P., Blaney, D., Hutchinson, I., 2017. Basalt–trachybasalt samples in gale crater, Mars. Meteoritics Planet Sci. 52. https://doi.org/10.1111/maps.12953, 2931–2410.

Ehlmann, B.L., Mustard, J.F., Swayze, G.A., Clark, R.N., Bishop, J.L., Poulet, F., Des Marais, D.J., Roach, L.H., Milliken, R.E., Wray, J.J., Barnouin-Jha, O., Murchie, S.L., 2009. Identification of hydrated silicate minerals on Mars using MRO-CRISM: geologic context near Nili Fossae and implications for aqueous alteration. J. Geophys. Res. 114, E00D08. https://doi.org/10.1029/2009JE003339.

Ehlmann, B., Mustard, J.F., Murchie, S.L., Poulet, F., Bishop, J.L., Brown, A.J., Calvin, W.M., Clark, R.N., Des Marais, D.J., Milliken, R.E., Roach, L.H., Roush, T.L., Swayze, G.A., Wray, J.J., 2008. Orbital identification of carbonate-bearing rocks on Mars. Science 322, 1828–1832.

Ehlmann, B.L., Mustard, J.F., Clark, R.N., Swayze, G.A., Murchie, S.L., 2011. Evidence for llow-grade metamorphism, hydrothermal alteration, and diagenesis on Mars from phyllosilicate mineral assemblages. Clay Clay Miner. 59, 259–377.

Einarsson, Th, 2005. Geology of Iceland – Rocks and Landscape. Translated to English by G. Douglas. Mal Og Menning Publisher, Reykjavik, p. 309.

Emeleus, C.H., Cheadle, M.J., Hunter, R.H., Upton, B.G.J., Wadsworth, W.J., 1996. The Rum layered suite. In: Cawthorn, Richard Grant (Ed.), Developments in Petrology, vol. 15. Elsevier, pp. 403–439.

Filiberto, J., Treiman, A.H., Giesting, P.A., Goodrich, C.A., Gross, J., 2014. High-temperature chlorine-rich fluid in the martian crust: a precursor to habitability. Earth Planet Sci. Lett. 401, 110–115. https://doi.org/10.1016/j.epsl.2014.06.003.

Flahaut, J., Mustard, J.~F., Quantin, C., Clenet, H., Allemand, P., Thomas, P., 2011. Dikes of distinct composition intruded into Noachian-aged crust exposed in the walls of Valles Marineris. Geophys. Res. Lett. 38. https://doi.org/10.1029/2011GL048109.

Flahaut, J., Carter, J., Poulet, F., Bibring, J.-P., van Westrenen, W., Davies, G.R., Murchie, S.L., 2015. Embedded clays and sulfates in Meridiani Planum, Mars. Icarus 248, 269–288. J.-P.

French, B.M., 1998. Traces of catastrophe. A handbook of shock-metamorphic effects in terrestrial meteorite impact structures. Lunar Planet. Inst. Contr. 954, 120.

French, B.M., Koeberl, C., Gilmour, I., Shirley, S.B., Dons, A., Naterstad, J., 1997. The Gardnos impact structure, Norway: petrology and geochemistry of target rocks and impactites. Geochim. Cosmochim. Acta 61, 873–904.

Furnes, H., Pedersen, R.B., Stillman, C.J., 1988. The Leka Ophiolite complex, central Norwegian Caledonides. Field characteristics and geotectonic significance. J. Geol. Soc. 145, 401–412. London.

Gendrin, A., Mangold, N., Bibring, J.-P., Langevin, Y., Gondet, B., Poulet, F., Bonello, G., Quantin, C., Mustard, J., Arvidson, R., LeMouélic, S., 2005. Sulfates in martian layered terrains: the OMEGA/Mars express view. Science 307 (5715), 1587–1591.

Gibson, R.L., Reimold, W.U., 2008. Geology of the Vredefort Impact Structure. Pretoria Council of Geoscience, p. 180.

Goderis, S., Kalleson, E., Tagle, R., Dypvik, H., Schmitt, R.T., Erzinger, J., Clayes, P., 2009. A non-magmatic iron projectile for the Gardnos impact event. Chem. Geol. 258, 145–156.

Gohn, G.S., Koeberl, C., Miller, K.G., Reimold, W.U., 2009. The ICDP-USGS deep drilling project in the Chesapeake Bay impact structure: results from the Eyreville core holes. Geol. Soc. Am. Spec. Pap. 458, 975.

Goudge, T.A., Mustard, J.F., Head, J.W., Fassett, C.I., 2012. Constraints on the history of open-basin lakes on Mars from the composition and timing of volcanic resurfacing. J. Geophys. Res. (Planets) 117. https://doi.org/10.1029/2012JE004115.

Hellevang, H., Dypvik, H., Kalleson, E., Pittarello, L., Koeberl, C., 2013. Can alteration experiments on impact melts from El'gygytgin and volcanic glass shed new light on the formation of the martian surface? Meteorit. Planet. Res. 48, 1287–1295.

Hewins, R.H., Zanda, B., Humayun, M., Nemchin, A., Lorand, J.-P., Pont, S., Deldicque, D., Bellucci, J.J., Beck, P., Leroux, H., Marinova, M., Remusat, L., Göpel, C., Lewin, E., Grange, M., Kennedy, A., Whitehouse, M.J., 2017. Regolith breccia Northwest Africa 7533: mineralogy and petrology with implications for early Mars. Meteoritics Planet Sci. 52, 89–124. https://doi.org/10.1111/maps.12740.

Horgan, B.H.N., Anderson, R.B., Dromart, G., Amador, E.S., Rice, M.S., 2020. The mineral diversity of Jezero crater: evidence for possible lacustrine carbonates on Mars. Icarus 339, 115326.

Howard, A.D., Moore, J.M., Rossman, P.I., 2005. An intense terminal epoch of widespread fluvial activity on early Mars: 1. Valley network incision and associated deposits. J. Geophys. Res. 110 (E12). CiteID E12S14.

Hudson-Edwards, K.A., Schell, C., Macklin, M.G., 1999. Mineralogy and geochemistry of alluvium contaminated by metal mining in the Rio Tinto area, southwest Spain. Appl. Geochem. 14, 1015–1030.

Humayun, M., 2013. Origin and age of the earliest Martian crust from meteorite NWA 7533. Nature 503. https://doi.org/10.1038/nature12764.

Irvine, T.N., Baragar, W.R.A., 1971. A guide to the chemical classification of the common volcanic rocks. Can. J. Earth Sci. 8, 523–548.

Ivanov, B., Deutsch, A., 2002. The phase diagram of $CaCO_3$ in relation to shock compression and decomposition. Phys. Earth Planet. In. 129, 131–143.

Jerram, D.A., Davis, G.R., Mock, A., Charrier, A., Marsh, B.D., 2010. Quantifying 3D crystal populations, packing and layering in shallow intrusions: a case study from the Basement Sill, Dry Valleys, Antarctica. Geosphere 6 (5), 537–548.

Jourdan, F., Moynier, F., Koeberl, C., Eroglu, S., 2011. 40Ar-39Ar age of Lonar crater and consequence for the geochronology of planetary impacts. Geology 39, 671–674.

Kalleson, E., 2009. The Gardnos structure; the impactites, sedimentary deposits and post-impact history. PhD theses. Fac. Math Nat.Sci, Univ. Oslo 868, 1–202. ISSN 1501-7710.

Kalleson, E., Corfu, F., Dypvik, H., 2009. U-Pb systematics of zircón and titanite from the Gardnos impact structure, Norway: evidence for impact at 546 Ma. Geochem. Cosmochim. Acta 73, 3077–3092.

Kalleson, E., Dypvik, H., Nilsen, O., 2010. Melt-bearing impactites (suevite and impact melt rock) within the Gardnos strcuture, Norway. Meteoritics Planet Sci. 45, 798–827.

Klingelhöfer, G., Morris, R.V., Bernhardt, B., Schröder, C., Rodionov, D.S., de Souza, P.A., Yen, A., Gellert, R., Evlanov, E.N., Zubkov, B., Foh, J., Bonnes, U., Kankeleit, E., Gütlich, P., Ming, D.W., Renz, F., Wdowiak, T., Squyres, S.W., Arvidson, R.E., 2004. Jarosite and hematite at Meridiani Planum from Opportunity's Mössbauer spectrometer. Science 306 (5702), 1740–1745, 2004.

Korablev, O.I., 17 co-authors, 2017. Infrared Spectrometer for ExoMars (ISEM), a mast-mounted instrument for the rover. Astrobiol. J. 17 (6–7), 542–564.

Krzesińska, A.M., Bultel, B., Viennet, J.C., Werner, S.C., 2019. Experimental constraints on the formation of vermiculitic, Fe, Mg-phyllosilicates on Mars with relevance to the aqueous history of Oxia Planum. LPI Contributions 2089, 6216.

Krzesińska, A.M., Bultel, B., Loizeau, D., Craw, D., April, R., Poulet, F., Werner, S.C., 2021. Mineralogical and spectral (NIR) characterization of Fe-rich vermiculite-bearing terrestrial deposits and constraints for mineralogy of Oxia Planum, ExoMars 2022 landing site. Astrobiology 21 (8), 997–1016. https://doi.org/10.1089/ast.2020.2410.

Lafuente, B., Downs, R.T., Yang, H., Stone, N., 2015. The power of databases: the RRUFF Project. In: Armbruster, T., Danisi, R.M. (Eds.), Highlights in Mineralogical Crystallography (Book), first ed. Publisher: De Gruyter, Berlin, pp. 1–30.

Lantz, C., Poulet, F., Loizeau, D., Pilorget, C., Carter, J., Werner, S.C., Dypvik, H., Rull, F., Veneranda, M., 2020. Planetary Terrestrial Analogues Library (PTAL) project: 1. Characterization of samples by NIR point spectrometer. Planet. Space Sci. 189, 18 article id. 104989.

Lee, M.R., Tomkinson, T., Hallis, L.J., Mark, D.F., 2015. Formation of iddingsite veins in the martian crust by centripetal replacement of olivine: evidence from the nakhlite meteorite Lafayette. Geochem. Cosmochim. Acta 154, 49–65.

Lodders, K., 1998. A survey of shergottites, nahklite and chassigny meteorites whole-rock compositions. Meteoritics Planet Sci. 33, A183–A190.

Loizeau, D., Lequertier, G., Poulet, F., Hamm, V., Pilorget, C., Meslier-Lourit, L., Lantz, C., Werner, S., Rull, F., Bibring, J.-P., 2020. Planetary terrestrial analogues library (PTAL) project: 2. Building a laboratory setup for Micromega characterization. Planet. Space Sci. 193, 105087. https://doi.org/10.1016/j.pss.2020.105087.

Loizeau, D., and et al. (submitted). Planetary Terrestrial Analogues Library Project: 3. Characterization of Samples with MicrOmega. Submitted to Astrobiology.

Lopez-Reyes, G., Rull Pérez, F., 2017. A method for the automated Raman spectra acquisition. J. Raman Spectrosc. 48 (11), 1654–1664.

Lopez-Reyes, G., Saiz, J., Guzmán, Á., Moral, A., Pérez, C., Rull, F., Manrique, J.A., Medina, J., 2018. RLS FM performance characterization and calibration campaign with the Instrument Data Analysis Tool (IDAT). Eur. Planet. Sci. Congr. 1132, 2018.

Lopez-Reyes, G., Veneranda, M., Martin, A.G., Manrique, J.A., Moral, A., Perez-Canora, C., Prieto, J.A.R., Arranz, A.S., Saiz, J., Lalla, E., Konstantinidis, M., Ballesteros, O.P., Medina, J., Gonzalez, M.A., Charro, E., Lopez, J.M., Calzada, L.M.N., and F. Rull, in review.; The Raman laser spectrometer ExoMars simulator (RLS Sim): a heavy-duty Raman tool for ground testing on ExoMars). J. Raman Spectrosc..

C. Mandon, L., Quantin- Nataf, C., Thollot, P., Mangold, N., Lozac'h, L., Dromart, G., Beck, P., Dehouck, E., Breton, S., Millot, C., Volat, M., 2020. Refining the age, emplacement and alteration scenarios of the olivine-rich unit in the Nili Fossae region, Mars Icarus 336, 113436.

Marti, J., Mitjavila, J., Arana, V., 1994. Stratigraphy, structure and geochronology of the Las Canadas caldera (Tenerife, canary islands). Geol. Mag. 131, 715–727.

Martinez-Frias, J., Delgado - Huertas, A., Garcia-Moreno, F., Reyes, E., Lunar, R., Rull, F., 2007. Isotopic signatures of extinct low-temperature hydrothermal chimneys in the Jaroso Mars analog. Planet. Space Sci. 55, 441–448.

Martinez-Frias, J., Lunar, R., Rodriguez-Losada, J.A., Delgado, A., Rull, F., 2004. The volcanism-related multistage hydrothermal system of El Jaroso (SE Spain): implication for the exploration of Mars. Earth Planets Space 46, 5–8.

Massé, M., et al., 2008. Mineralogical composition, structure, morphology, and geological history of Aram Chaos crater fill on Mars derived from OMEGA Mars Express data. J. Geophys. Res. (Planets) 113. https://doi.org/10.1029/2008JE003131.

Maurice, S., et al., 2012. The ChemCam instrument suite on the Mars science laboratory (MSL) rover: science objectives and mast unit description. Space Sci. Rev. 170, 95–166. https://doi.org/10.1007/s11214-012-9912-2.

McCubbin, F.M., Boyce, J.W., Srinivasan, P., Santos, A.R., Elardo, S.M., Filiberto, J., Steele, A., Shearer, C.K., 2016. Heterogeneous distribution of H2O in the Martian interior: implications for the abundance of H2O in depleted and enriched mantle sources. Meteoritics Planet Sci. 51, 2036–2060.

McDougall, I., 1976. Geochemistry and origin of basalt of the Columbia River group, Oregon and Washington. Geol. Soc. Am. Bull. 87, 777–792.

McSween, H.Y., Taylor, G.J., Wyatt, M.B., 2009. Elemental composition of the martian crust. Science 324, 736–739. https://doi.org/10.1126/science.1165871.

Meunier, A., Petit, S., Ehlmann, B.L., Dudoignon, P., Westall, F., Mas, A., El Albani, A., Ferrage, E., 2012. Magmatic precipitation as a possible origin of Noachian clays on Mars. Nat. Geosci. 5, 739.

Michalski, J.R., Niles, P.B., 2010. Deep crustal carbonate rocks exposed by meteor impact on Mars. Nat. Geosci. 3, 751–755. https://doi.org/10.1038/ngeo971.

Michalski, J.R., Cuadros, J., Bishop, J.L., Darby Dyar, M., Dekov, V., Fiore, S., 2015. Constraints on the crystal-chemistry of Fe/Mg-rich smectitic clays on Mars and links to global alteration trends. Earth Planet Sci. Lett. 427, 215–225. https://doi.org/10.1016/j.epsl.2015.06.020.

Michalski, J.R., et al., 2017. Shock metamorphism of clay minerals on Mars by meteor impact. Geophys. Res. Lett. 44, 6562–6569. https://doi.org/10.1002/2017GL073423.

Mittlefehldt, D.W., 1994. ALH84001, a cumulate orthopyroxenite member of the martian meteorite clan. Meteorit. Planet. Sci. 29, 214–221.

Morris, R.V., 12 colleagues, 2010. Identification of carbonate-rich outcrops on Mars by the Spirit rover. Science 329, 421. https://doi.org/10.1126/science.1189667.

Moyano-Cambero, C.E., Trigo-Rodríguez, J.M., Benito, M.I., Alonso-Azcárate, J., Lee, M.R., Mestres, N., Martínez-Jiménez, M., Martín-Torres, F.J., Fraxedas, J., 2017. Petrographic and geochemical evidence for multiphase formation of carbonates in the Martian orthopyroxenite Allan Hills 84001. Meteoritics Planet Sci. 52, 1030–1047.

Murchie, S.L., 17 colleagues, 2009. A synthesis of Martian aqueous mineralogy after one Mars year of observations from the Mars Reconnaissance Orbiter. J. Geophys. Res. 114, E00D06.
Mustard, J.F., Poulet, F., Gendrin, A., Bibring, J.-P., Langevin, Y., Gondet, B., Mangold, N., Bellucci, G., Altieri, F., 2005. Olivine and pyroxene diversity in the crust of Mars. Science 307 (5715), 1594–1597.
Mustard, J.F., Murchie, S.L., Pelkey, S.M., Ehlmann, B.L., Milliken, R.E., Grant, J.A., Bibring, J.-P., Poulet, F., Bishop, J., Dobrea, E.N., Roach, L., Seelos, F., Arvidson, R.E., Wiseman, S., Green, R., Hash, C., Humm, D., Malaret, E., McGovern, J.A., Seelos, K., Clancy, T., Clark, R., Marais, D.D., Izenberg, N., Knudson, A., Langevin, Y., Martin, T., McGuire, P., Morris, R., Robinson, M., Roush, T., Smith, M., Swayze, G., Taylor, H., Titus, T., Wolff, M., 2008. Hydrated silicate minerals on Mars observed by the Mars reconnaissance orbiter CRISM instrument. Nature 454 (7202), 305–309.
Nachon, M., 35 colleagues, 2014. Calcium sulfate veins characterized by ChemCam/Curiosity at Gale crater, Mars. J. Geophys. Res. (Planets) 119, 1991–2016. https://doi.org/10.1002/2013JE004588.
Neumann, E.R., Larsen, B.T., Sundvoll, B., 1985. Compositional variations among gabbroic intrusions in the Oslo rift. Lithos 18, 35–59.
Newsom, H.E., 1980. Hydrothermal alteration of impact melt sheets with implication for Mars. Icarus 44, 207–216.
F. Ody, A., Poulet, F., Langevin, Y., Bibring, J.-P., Bellucci, G., Altieri, B., Gondet, B., Vincendon, M., Carter, J., Manaud, N., 2012. Global maps of anhydrous mineral at the surface of Mars from OMEGA/MEx J. Geophys. Res. 117 (E11). https://doi.org/10.1029/2012JE004117.
Osinski, G.R., Tornabene, L.L., Banerjee, N.R., Cockell, C.S., Flemming, R., Izawa, M.R.M., Mc Cutcheon, J., Parnell, J., Preston, L.J., Pickergill, A.E., Pontefract, A., Sapers, H.M., Southam, G., 2013. Impact generated hydrothermal systems on Earth and Mars. Icarus 224, 347–363.
Pan, L., Quantin-Nataf, C., Breton, S., Michaut, C., 2019. The impact origin and evolution of Chryse Planitia on Mars revealed by buried craters. Nat. Commun. 10. https://doi.org/10.1038/s41467-019-12162-0.
Papike, J.J., Karner, J.M., Shearer, C.K., Burger, P.V., 2009. Silicate mineralogy of martian meteorites. Geochem. Cosmochim. Acta 73 (24), 7443–7485.
Poag, C.W., Koeberl, C., Reimold, W.U., 2004. The Chesapeake Bay Crater: Geology and Geophysics of a Late Eocene Submarine Impact Structure. Springer –Verlag, 522p, with CD-ROM.
Poulet, F., Erard, S., 2004. Nonlinear spectral mixing: quantitative analysis of laboratory mineral mixtures. J. Geophys. Res. Planets 109 (E2), 12.
Poulet, F., Bibring, J.-P., Mustard, J.F., Gendrin, A., Mangold, N., Langevin, Y., Arvidson, R.E., Gondet, B., Gomez, C., Berthé, M., Bibring, J.-P., Langevin, Y., Erard, S., Forni, O., Gendrin, A., Gondet, B., Manaud, N., Poulet, F., Poulleau, G., Soufflot, A., Combes, M., Drossart, P., Encrenaz, T., Fouchet, T., Melchiorri, R., Bellucci, G., Altieri, F., Formisano, V., Fonti, S., Capaccioni, F., Cerroni, P., Coradini, A., Korablev, O., Kottsov, V., Ignatiev, N., Titov, D., Zasova, L., Mangold, N., Pinet, P., Schmitt, B., Sotin, C., Hauber, E., Hoffmann, H., Jaumann, R., Keller, U., Arvidson, R., Mustard, J., Forget, F., 2005. The Omega Team, 2005. Phyllosilicates on Mars and implications for early martian climate. Nature 438, 623–627. https://doi.org/10.1038/nature04274.
Poulet, F., Mangold, N., Platevoet, B., Bardintzeff, J.M., Sautter, V., Mustard, J.F., Bibring, J.P., Pinet, P., Langevin, Y., Gondet, B., Aléon-Toppani, A., 2009. Quantitative compositional analysis of martian mafic regions using the MEx/OMEGA reflectance data: 2. Petrological implications. Icarus 201, 84–101.
Rapin, W., 9 colleagues, 2015. Hydration state of calcium sulfate veins as observed by the ChemCam instrument. In: Lunar and Planetary Science Conference, 2015.
Retallack, G.J., 2008. Cenozoic cooling and grassland expansion in Oregon and Washington. PaleoBios 28, 89–113.
Retallack, G.J., Bestland, E.A., Fremd, T.J., 2000. Eocene and Oligocene Paleosols of Central Oregon, vol. 344. Geological Society of America, Special Paper, p. 191.
Riu, L., Poulet, F., Bibring, J.-P., Gondet, B., 2019. The M3 project: 2 - global distributions of mafic mineral abundances on Mars. Icarus 322, 31–53.
Rull, F., Martinez-Frias, J., Medina, J., 2005. Surface mineral analysis from two possible Martian analogs (Rio Tinto and Jaroso Ravine) using micro-, macro- and remote laser Raman spectroscopy. Geophys. Res. Abstr. 7.
Rull, F., Maurice, S., Hutchinson, I., Moral, A., Perez, C., Diaz, C., Colombo, M., Belenguer, T., Lopez-Reyes, G., Sansano, A., Forni, O., Parot, Y., Striebig, N., Woodward, S., Howe, C., Tarcea, N., Rodriguez, P., Seoane, L., Santiago, A., Rodriguez-Prieto, J.A., Medina, J., Gallego, P., Canchal, R., Santamaría, P., Ramos, G., Vago, J.L., 2017. The Raman laser spectrometer for the ExoMars rover mission to Mars. Astrobiology 17, 6–7.
Sætre, C., Hellevang, H., Riu, L., Dypvik, H., Pilogret, C., Poulet, F., Werner, S.C., 2018. Experimental hydrothermal alteration of basaltic glass with relevance to Mars. Meteoritics Planet Sci. 54, 357–378.
Santos, A.R., Agee, C.B., McCubbin, F.M., Shearer, C.K., Burger, P.V., Tartèse, R., Anand, M., 2015. Petrology of igneous clasts in Northwest Africa 7034: implications for the petrologic diversity of the martian crust. Geochem. Cosmochim. Acta 157, 56–85.
Sautter, V., Toplis, M.J., Cousin, A., Gasnault, O., Maurice, S., Lasue, J., Meslin, P.Y., Oinet, P., Rapin, W., Wiens, R.C., Lanza, N., Clegg, S., Fabre, C., Ollila, A., Bridges, J.C., Magnold, N., Le Deit, L., Le Mouelic, S., Fisk, M., Beck, P., Stolper, E.M., Newsom, H., Dyar, D., Vaniman, D., Wray, J.J., 2015. In situ evidence for continental crust on early Mars. Nat. Geosci. 8. https://doi.org/10.1038/ngeo2474.
Sautter, V., Toplis, M.J., Beck, P., Mangold, N., Wiens, R., Pinet, P., Cousin, A., Maurice, S., LeDeit, L., Hewins, R., Gasnault, O., Quantin, C., Forni, O., Newsom, H., Meslin, P.-Y., Wray, J., Bridges, N., Payre, V., Rapin, W., Le Mouelic, S., 2016. Magmatic complexity on early Mars as seen through a combination of orbital, in-situ and meteorite data. Lithos 254, 36–52. https://doi.org/10.1016/j.lithos.2016.02.023.
Sengupta, D., Bhandari, N., Watanabe, S., 1997. Formation age of lonar meteor crater, India. Rev. Fis. Apl. Instrumentacao 12, 1–7.
Senthil Kumar, P., Prasanna Lakshmi, K.J., Krishna, N., Menon, R., Sruthi, U., Keerthi, V., Senthil Kumar, A., Mysaiah, D., Seshunarayana, T., Sen, M.K., 2014. Impact fragmentation of Lonar crater, India: implications for impact cratering processes in basalt. J. Geophys. Res. Planets 119, 2029–2059.
Sheldon, N.D., 2003. Pedogenesis and geochemical alteration of the picture Gorge subgroup, Columbian River basalt, Orgeon. Geol. Soc. Am. Bull. 115, 1377–1387.
Sigmarsson, O., Steinthorsson, S., 2007. Origin of Icelandic basalts: a review of their petrology and geochemistry. J. Geodyn. 43, 87–100.
Skok, J.R., Mustard, J.F., Tornabene, L.L., Pan, C., Rogers, D., Murchie, S.L., 2012. A spectroscopic analysis of Martian crater central peaks: formation of the ancient crust. J. Geophys. Res. Planets 117, 33pp. https://doi.org/10.1029/2012JE004148.
Squyres, S.W., Knoll, A.H., 2005. Sedimentary rocks at Meridiani Planum: origin, diagenesis, and implications for life on Mars. Earth Planet Sci. Lett. 240, 1–10. https://doi.org/10.1016/j.epsl.2005.09.038.
Squyres, S.W., et al., 2012. ancient impact and aqueous processes at Endeavour crater, Mars. Science 336, 570. https://doi.org/10.1126/science.1220476.
Tanaka, K.L., Robbins, S.J., Fortezzo, C.M., Skinner, J.A., Hare, T.M., 2014. The digital global geologic map of Mars: chronostratigraphic ages, topographic and crater morphologic characteristics, and updated resurfacing history. Planet. Space Sci. 95, 11–24.
Taylor, G.J., 2013. The bulk composition of Mars. Chemie der Erde - Geochemistry 73 (4), 401–420.
Thollot, P., 9 colleagues, 2012. Most Mars minerals in a nutshell: various alteration phases formed in a single environment in Noctis Labyrinthus. J. Geophys. Res. Planets 117, 28. https://doi.org/10.1029/2011JE004028.
Tornabene, L.L., 6 colleagues, 2013. An impact origin for hydrated silicates on Mars: a synthesis. J. Geophys. Res. Planets 118, 994–1012. https://doi.org/10.1002/jgre.20082.
Treiman, A.H., Amundsen, H.E.F., Blake, D.F., Bunch, T., 2002. Hydrothermal origin for carbonate globules in Martian meteorite ALH84001: a terrestrial analogue from Spitsbergen (Norway). Earth Planet Sci. Lett. 204 (3–4), 323–332.
Troll, V.R., Walter, T.R., Schmincke, H.U., 2002. Cyclic Caldera collapse: piston or piecemeal subsidence? Field and experimental evidence. Geology 30, 135–138.
Troll, V.R., Carracedo, J.-C., 2016. The Geology of the Canary Islands. Elsevier, p. 636. ISBN 9780128096642.
Trønnes, R.G., Baron, M.A., Eigenmann, K.R., Guren, M.G., Heyn, B.H., Løken, A., Mohn, C.E., 2019. Core formation, mantle differentiation and core-mantle interaction within Earth and the terrestrial planets. Tectonophysics 760, 165–198.
Udry, A., Howarth, G.H., Lapen, T.J., Righter, M., 2017. Petrogenesis of the NWA 7320 enriched martian gabbroic shergottite: insight into the martian crust. Geochem. Cosmochim. Acta 204, 1–18.
Valley, J.W., Eiler, J.M., Graham, C.M., Gibson, E.K., Romanek, C.S., Stolper, E.M., 1997. Low-temperature carbonate concretions in the martian meteorite ALH84001: evidence from stable isotopes and mineralogy. Science 275, 1633–1638.
Veneranda, M., Sáiz, J., Sanz-Arranz, A., Manrique, J.A., Lopez-Reyes, G., Medina, J., Dypvik, H., Werner, S.C., Rull, F., 2019 a. Planetary terrestrial analogues library (PTAL) project: Raman data overview. J. Raman Spectrosc. (1), 1–19, 2019.
Veneranda, M., Manrique-Martinez, J.A., Lopez-Reyes, G., Medina, J., Torre-Fdez, I., Castro, K., Madariaga, J.M., Lantz, C., Poulet, F., Krzesińska, A.M., Hellevang, H., Werner, S.C., Rull, F., 2019b. Spectroscopic study of olivine-bearing rocks and its relevance to the ExoMars rover mission. Spectrochim. Acta Mol. Biomol. Spectrosc. 223, 11736.
Veneranda, M., Saiz, J., Lopez-Reyes, G., Manrique, J.A., Sanz-Aurelio, A., Garcia-Prieto, C., Werner, S.C., Moral, A., Madariaga, J.M., Rull, F., 2020. PTAL , ADAMM and SpectPro : novel tools to support ExoMars and Mars 2020 science operations. Europlanet Sci. Congr. 2020.
Veneranda, M., Lopez-Reyes, G., Pascual Sanchez, E., Krzesińska, A.M., Manrique-Martinez, J.A., Sanz-Arranz, A., Lantz, C., Lalla, -E., Moral, A., Medina, J., Poulet, F., Dypvik, H., Werner, S.C., Vago, J.L., Rull, F., 2021. ExoMars Raman laser spectrometer: a tool to Semiquantify the Serpentinization degree of olivine-rich rocks on Mars. Astrobiology 21.
Viennet, J.-C., Bultel, B., Riu, L., Werner, S.C., 2017. Dioctahedral phyllosilicates versus zeolites and carbonates versus zeolites competitions as constraints to understanding early Mars alteration conditions. J. Geophys. Res. Planets 122, 2328–2343. https://doi.org/10.1002/2017JE005343.
Viennet, J.-C., Bultel, B., Werner, S.C., 2019a. Experimental reproduction of the martian weathering profiles argues for a dense Noachian CO2 atmosphere. Chem. Geol. 525, 82–95. https://doi.org/10.1016/j.chemgeo.2019.07.009.
Viennet, J.-C., Bernard, S., Le Guillou, C., Jacquemot, P., Balan, E., Delbes, L., Rigaud, B., Georgelin, T., Jaber, M., 2019b. Experimental clues for detecting biosignatures on Mars. Geochem. Perspect. Lett. 2019 (11), 28–33. https://doi.org/10.7185/geochemlet.1931.
Viennet, J.-C., Bernard, S., Le Guillou, C., Sautter, S., Schmitt-Kopplin, P., Beyssac, O., Pont, S., Zanda, B., Edwin, R., Remusat, R., 2020. Tardi-magmatic precipitation of Martian Fe/Mg-rich clay minerals via igneous differentiation. Geochem. Perspect. Lett. 47–52. https://doi.org/10.7185/geochemlet.2020, 2020.
Warren, P.H., 1998. Petrologic evidence for low-temperature, possibly flood evaporitic origin of carbonates in the ALH84001 meteorite. J. Geophys. Res. 103 (E7), 16759–16773.
Waters, A.C., 1961. Stratigraphic and lithologic variations in the Columbia River basalt. Am. J. Sci. 259, 583–611.

Weitz, C.M., Bishop, J.L., Thollot, P., Mangold, N., Roach, L.H., 2011. Diverse mineralogies in two troughs of Noctis Labyrinthus, Mars. Geology 39 (10), 899–902.

Wiens, R.C., 79 colleagues, 2012. the ChemCam instrument suite on the Mars science laboratory (MSL) rover: Body unit and combined system tests. Space Sci. Rev. 170, 167–227. https://doi.org/10.1007/s11214-012-9902-4.

Wiens, R.C., Maurice, S., Lasue, J., Forni, O., Anderson, R.B., Clegg, S., Bender, S., Blaney, D., Barraclough, B.L., Cousin, A., Deflores, L., Delapp, D., Dyar, M.D., Fabre, C., Gasnault, O., Lanza, N., Mazoyer, J., Melikechi, N., Meslin, P.-Y., Newsom, H., Ollila, A., Perez, R., Tokar, R.L., Vaniman, D., 2013. Pre-flight calibration and initial data processing for the ChemCam laser-induced breakdown spectroscopy instrument on the Mars Science Laboratory rover. Spectrochim. Acta B Atom Spectrosc. 82, 1–27.

Wiens, R.C., Maurice, S., Perez, F., 2017. The SuperCam Remote Sensing Instrument Suite for the Mars 2020 Rover. A Preview, 2017. http://www.spectroscopyonline.com/supercam- remote-sensing-instrument-suite-mars-2020-rover-preview.

Williams, R.M.E., Grotzinger, J.P., Dietrich, W.E., Gupta, S., Sumner, D.Y., Wiens, R.C., Mangold, N., Malin, M.C., Edgett, K.S., Maurice, S., Forni, O., Gasnault, O., Ollila, A., Newsom, H.E., Dromart, G., Palucis, M.C., Yingst, R.A., Anderson, R.B., Herkenhoff, K.E., Le Mouélic, S., Goetz, W., Madsen, M.B., Koefoed, A., Jensen, J.K., Bridges, J.C., Schwenzer, S.P., Lewis, K.W., Stack, K.M., Rubin, D., Kah, L.C., Bell III, J.F., Farmer, J.D., Sullivan, R., Van Beek, T., Blaney, D.L., Pariser, O., Deen, R.G., MSL Science Team, 2013. Martian fluvial conglomerates at gale crater. Science 340 (6136), 1068–1072.

Wray, J.J., Hansen, S.T., Dufek, J., Swayze, G.A., Murchie, S.L., Seelos, F.P., Skok, J.R., Irwin III, R.P., Ghiorso, M.S., 2013. Prolonged magmatic activity on Mars inferred from the detection of felsic rocks. Nat. Geosci. 6, 1013–1017.